Experimental Preparation of Microcellular Polymer Blend Foams by Exploiting Structural non-Homogeneity

Dominik Kohlhoff

2012

Submitted to the Graduate School of Engineering

for the degree of

Doctor of Engineering

Kyoto University

Department of Chemical Engineering

Materials Process Engineering Division

July 2012

Contents

Chapter 1

General Introduction

1.1. Introductory Remarks

The term “plastic materials” is frequently used for high-molecular polymers which can be manufactured in many different ways due to their formability. Therefore, polymers are among the most coveted materials in these days. The fact that they can be shaped at lower temperatures than metals and their relatively low cost make them more promising than traditionally- used materials such as wood, glass, ceramics, etc.[1]

Since the global market for polymers is growing steadily,[2] a manifold of processing techniques related to reforming of plastic material exists. These techniques can be divided into primary and secondary shaping methods. Among the primary shaping methods are, for example, extrusion and injection molding. During extrusion, neat polymers or blends, i.e., systems consisting of two or more polymers, are in the molten state and mechanically pumped through a die into a profile of any shape such as a plate or a tube for further processing. Contrary to that, the injection molding process is used to manufacture the end product directly from the melt and the polymeric starting material, respectively. The melt is forced into a cavity having the shape of the desired end product and it remains there until solidification. The cavity is opened afterwards and the next batch can be prepared. Today, injection molding is among the most applied polymer processing methods and more than 30 % of all thermoplastic components are injection molded.[3]

The production steps following the extrusion process are known as secondary shaping methods. They are applied either after the polymer melt left extruder's die or after the sample already cooled down.

Further processing of the cooled samples can be done by thermoforming. Here, sheets of thermoplastic material are heated up to their softening temperature before they take up their new shapes of a cooled mould using vacuum, pressurized air, or a forming tool.[4]

Beside that, fiber spinning and blow molding are very common processes for extruded melts. The first method is used to manufacture fibers and lines. The molten polymer is forced vertically through several holes in a flat plate or a spinneret before the emerging threads are cross currently air cooled and stretched by winding them on a bobbin.[4] Nylon, e.g., is a very common material for fiber spinning.[5]

Blow molding is the most popular way of manufacturing hollow structures such as PET bottles and was borrowed from the glass industry.[6] A sleeve shaped parison of plastic is fixed between two mould halves, the halves are closed mechanically, and the sample is subsequently blown up with air. After solidification the sample is ejected and a new batch can be manufactured.[7- 8]

The aforementioned processes are commonly used to reshape the plastic material macroscopically. Contrary to that, foaming is a method to modify polymer matrix on micro or nano scale. It can be applied either during primary shaping, e.g. injection molding,[9] or in a subsequent step.[10]

1.2. Foaming of polymers and their blends

Polymeric materials which consist of a solid phase containing gas filled voids are called polymer foams. The solid phase can be a homopolymer or a blend consisting of two or more components and the gas phase can be generated in three different ways. Gas can be mixed with a polymer or a polymer solution[11] or blowing agents can be used which are either chemical or physical.[12] Each way of foaming polymers will be explained in detail in the following sections.

1.2.1. Foaming by mixing polymers and polymer solutions with gases

The mechanical mixing of polymers with gases is often used to create foams of natural as well as synthetic rubbers. Vieweg and Krekeler[11] summarized the experimental procedure briefly. Aqueous polymer solutions and aqueous dispersions are initially mixed with gas before gelation and hardening takes place. During the gelation step, water is removed by drying and a solid, foamed polymer can be obtained. Aqueous polymer solutions consisting of polyvinyl alcohol (PVA), e.g., are hardened by creating PVA polymer networks after mixing process.

1.2.2. Foaming with chemical blowing agents (CBA)

Chemical blowing agents can be classified into inorganic and organic substances and both types liberate gaseous components under certain thermal conditions. Solid inorganic blowing agents are, e.g., ammonium carbonate and carbonates of alkali metals such as sodium bicarbonate. These compounds are well known for a long time but two major disadvantages can be pointed out: Firstly, it is difficult to disperse the blowing agent homogeneously in the polymer matrix and secondly, the thermally

induced decomposition reactions are reversible.[13]

The advantage of using organic blowing agents instead of inorganic ones is the fact that thermal decompositions are irreversible; moreover, they can be dissolved homogeneously in the polymer. Well known substances in this field are, e. g., N- nitroso compounds, carbazides, and urea derivates.[14] Depending on the used CBA, the gaseous decomposition products can be, e.g., nitrogen (N_2) or ammonia (NH_3). Figure 1.1 displays irreversible, thermal decomposition of CBA schematically.

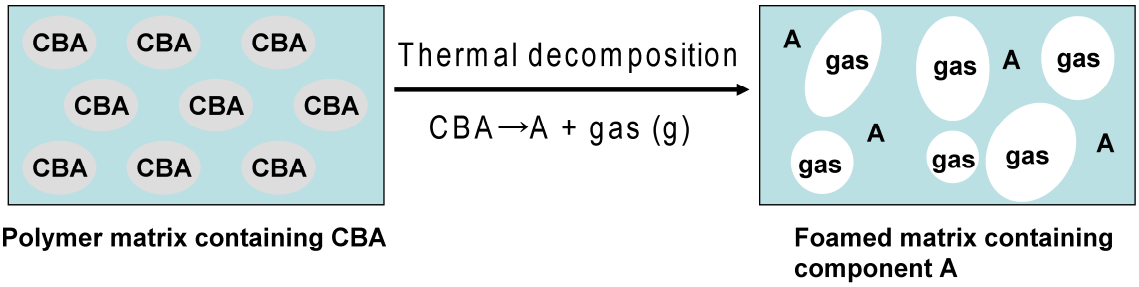

Figure 1.1. Scheme of a foaming process using a chemical blowing agent which decomposes irreversibly into residue A and a gaseous product.

1.2.3. Foaming with physical blowing agents (PBA)

Contrary to CBAs, physical blowing agents (PBA) can either be a gas or a volatile liquid with a low boiling point. They do not compose thermally, but their expandability is exploited. The large group of chlorofluorocarbons (CFC) such as trichlorofluoromethane (CFC- 11), dichlorodifluoromethane (CFC- 12), or 1, 2- dichloro- 1, 1, 2, 2- tetrafluoroethane (CFC- 114) belong to PBAs.[15] Since their negative impact on earth's stratospheric ozone layer is well known, the use of CFCs as possible blowing agents was drastically reduced. Components such as pentane and

hydrofluorocarbons (HCF)[16-17] were taken instead to overcome the phase- out of CFCs.

Behravesh et al.[16], e. g., used a mixture of PBA as well as CBA. They mixed polypropylene with isopentane and hydrocerol which consists of sodium bicarbonate and citric acid. The latter substance decomposed at elevated temperatures and liberated carbon dioxide (CO_2) as well as several other compounds, e.g. citraconic acid/ itaconic acid ($C_5H_6O_4$) and sodium carbonate (Na_2CO_3). CO_2 worked as primary blowing agent but was not sufficient to decrease the bulk foam density; therefore, the dissolved isopentane was used to diffuse into the CO_2 nucleated cells. An additional bubble nucleation by isopentane possibly occurred because the products of decomposed hydrocerol could induce heterogeneous nucleation.

Another approach of manufacturing polymer foams can be done by using blowing agents such as nitrogen or carbon dioxide.[17-19] These two blowing agents are among the environmentally most benign ones[20] and can be used for applications in the field of food industry, e. g. as food trays, and for medical applications.[21] The first experiments on creating gas infused microcellular foams were conducted approximately three decades ago when industrial needs for a reduce of polymeric packaging material increased.[17] Initial studies were done using amorphous polystyrene,[17] but the number of investigated polymers as well as polymer blends increased since that point of time: Baldwin et al.[22-23], e. g., used sheets of poly (ethylene terephthalate) (PET) and a PET resin containing polyolefin as nucleating agent. Here, differences in density and size of the foamed bubbles were determined for the investigated systems in the amorphous as well as in the semi-crystalline state.

Another research was done by Abu-Zahra et al.[24] They blended poly (vinyl chloride) (PVC) with several types of nanoclay, e. g., calcium montmorillonite clay and

magnesium lithium silicate clay, before an extrusion process for foaming was applied. Their experimental results were analyzed in terms of bulk foam density, bubbles sizes, bubble densities, and mechanical properties.

Since biopolymers from natural resources became more attractive and important in the last years,[25-26] several foaming experiments[26-27] with biomaterials were done, too.

The physical foaming process consists of two main steps. At first, the polymer is saturated with a gas under higher pressure. The benefits of the latter state are high solubility of gas, similar to organic solvents, the higher diffusivity of gas into the polymer as well as the significant reduction of glass transition temperature.[28-30] The subsequent step consists of cell nucleation and bubble growth. Therefore, a thermodynamic instability has to be created. This can either be done by a rapid pressure quench[18-19] or by an increase of temperature.[31] Figure 1.2. depicts the principle of aforementioned methods to create a thermodynamic instability. The gas sorption process can take place in the subcritical as well as in the supercritical state.

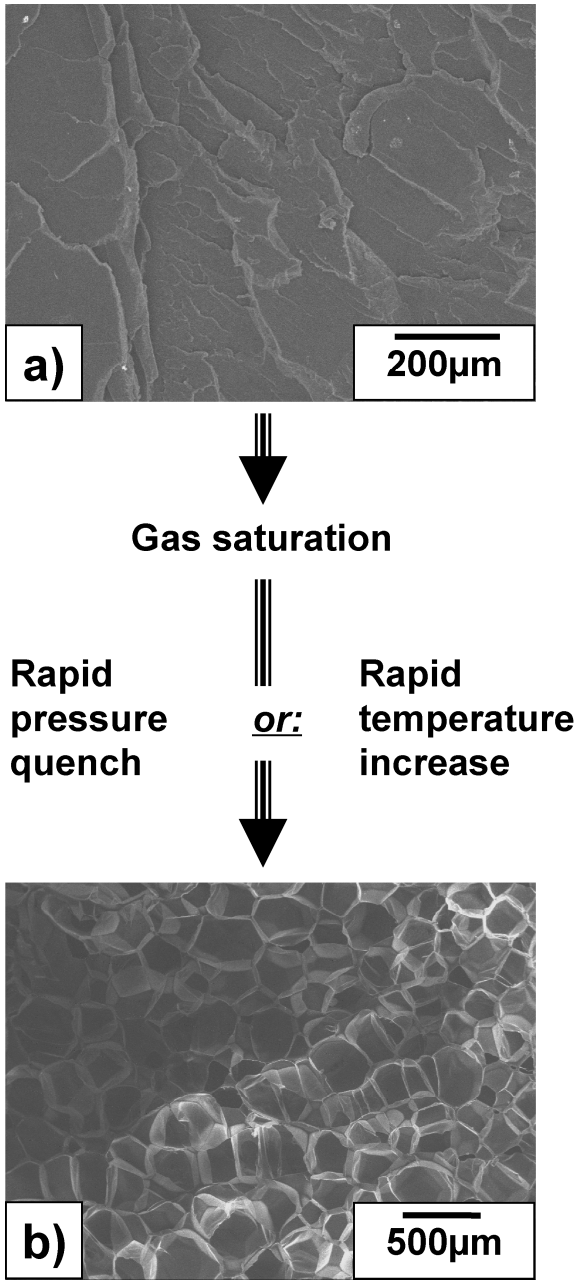

Figure 1.2. The principle of batch foaming with a PBA. Bubbles can nucleate and grow either by rapid gas expansion or by rapid decrease of gas` diffusivity as result of rapid temperature increase. Figure 1.2-a depicts the surface of a neat polymer (here: polystyrene) before gas saturation and Figure 1.2-b shows the polystyrene foam after rapid pressure quench from the supercritical state to atmospheric pressure.

1.3. Cell morphologies

Two characteristic cell morphologies can be obtained by foaming a polymeric specimen in the aforementioned ways. On the one hand it can happen that cell walls of the growing bubbles resist the occurring stress and do not rupture. In this case a closed cellular structure is generated. Zhu et al[32] explained this on the base of higher elasticity of the polymer matrix at foaming temperature. On the other hand it is possible that cell walls of growing bubbles are destroyed during bubble growth which can be caused by local differences in elasticity due to structural anisotropy,[34] different melting temperatures of crystalline polymers,[33] geometrical constraints, and induced shear forces acting during foaming on the polymer matrix which can be caused by a second phase, such as a polymer or dispersed particles in the matrix.[35] Foams with high open cell contents can be used as porous materials due to their high gas and liquid permeability. Ruckdäschel et al[35] summarized several ways of creating open- cellular foams as well as foams having bimodal cellular structures. Immiscible multiphase blends are crucial for creating aforementioned structures in one- step foaming processes.

Figure 1.3 displays examples of foams having a) closed and b) open cellular structures, respectively. It has to be pointed out that bubbles with non-ruptured cell walls even exist for high open cell contents.

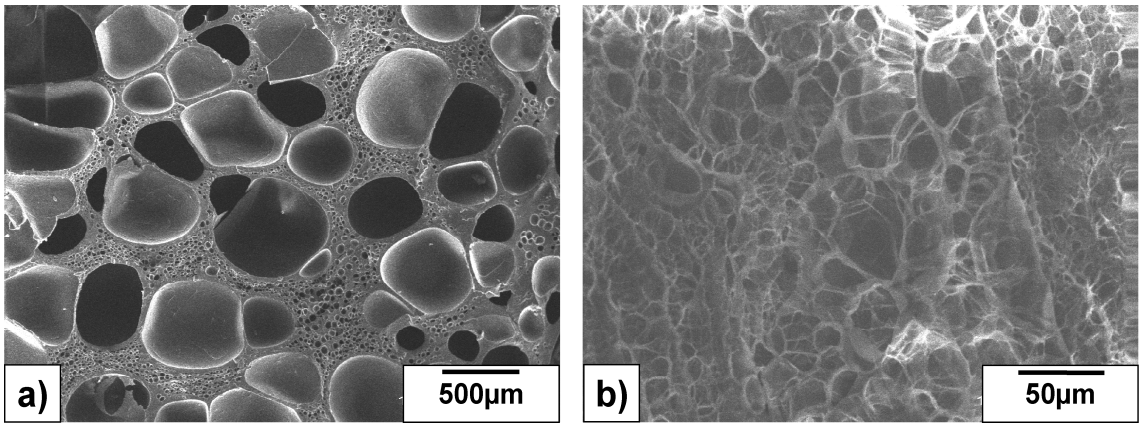

Figure 1.3. Morphology of foams with a) closed cellular structure and b) open cellular structure. Figure 1.3-a corresponds to a polystyrene- polymethyl methacrylate system and Figure 1.3-b corresponds to a poly-$_{L,D}$- lactic acid- polymethyl methacrylate system.

1.4. Miscibility of polymers

Miscibility and immiscibility of one polymer in another is a key factor of creating homogeneous and multiphase blends, respectively.[35] Two thermodynamic conditions must be fulfilled for a polymer- solvent or polymer- polymer system consisting of components A and B in order to be miscible. Firstly, Gibbs energy of mixing ΔG_{mix} which consists of temperature T, enthalpy of mixing ΔH_{mix}, and entropy of mixing ΔS_{mix} has to become zero or negative:[36]

$$\Delta G_{mix} = \Delta H_{mix} - T \cdot \Delta S_{mix} \leq 0. \quad (1)$$

Secondly, the second derivative of Gibbs energy with respect to volume fraction ϕ_B and the first derivative of the chemical potential $\Delta\mu_A$ of component A with respect to volume fraction ϕ_B has to be zero or positive:[36]

$$\left.\frac{\partial^2 \Delta G_{mix}}{\partial \phi_B^2}\right|_{T,p} = \frac{\partial \Delta \mu_A}{\partial \phi_B} \geq 0. \quad (2)$$

The Flory- Huggins lattice theory is a common approach to calculate changes in enthalpy and entropy.[37-38] This theory assumes polymer- solvent or polymer- polymer systems as three- dimensional lattices in which each lattice is occupied by a solvent molecule or polymer segment. Each moiety in a lattice can interact with neighbor lattices by exchanging energy. Applying this theory leads to the following equation for molar enthalpy of mixing $\Delta H_{mix,m}$:

$$\Delta H_{mix,m} = \chi RT\phi_A\phi_B. \quad (3)$$

Where R is the ideal gas constant, T the temperature, and χ the Flory- Huggins interaction parameter. Several methods exist to determine χ experimentally. Among them are osmotic pressure measurements, swelling equilibria, gas- liquid chromatography, and light scattering experiments.[39]

Furthermore, molar entropy of mixing $\Delta S_{mix,m}$ can be written as:

$$\Delta S_{mix,m} = -R\left(\frac{\phi_A}{X_A}\ln\phi_A + \frac{\phi_B}{X_B}\ln\phi_B\right). \quad (4)$$

Here, X_A and X_B are degrees of polymerization of each component and the molar Gibbs energy of mixing $\Delta G_{mix,m}$ according to equation (1) can be written as:[40]

$$\Delta G_{mix,m} = RT\left(\phi_A\phi_B\chi + \frac{\phi_A}{X_A}\ln\phi_A + \frac{\phi_B}{X_B}\ln\phi_B\right). \quad (5)$$

For high degrees of polymerization, the entropic term cannot compensate the enthalpy term if the interaction parameter χ is positive. Demixing takes place for most of the polymer blend systems.[41] Elias[42] mentioned that only a few polymer- polymer systems exist which do not demix. Among them are, e.g., poly(2,6- dimethyl- 1,4- phenyleneoxide)/ polystyrene at 200 °C. Miscibility of polymer blends generally can occur in the presence of strong attractive forces between the components such as dipole-dipole interactions and hydrogen bonds.[43]

1.5. Rheological characterization

To estimate which of the both aforementioned morphologies will occur during the foaming process, investigation on specimen's rheological properties in a certain range of temperatures and at the foaming temperature in particular is necessary. A detailed study for amorphous and semi-crystallline polymers was done by Liao and co-workers.[44-45]

1.5.1. Influence of elasticity on foamability and foam morphology

The elasticity of a homopolymer or polymer blend plays a significant role during foaming. Certain properties are essential to create foams with homogeneous morphologies. If elasticity of a specimen is too high at chosen foaming temperature, bubbles either nucleate only in some parts of the polymer or their growth is restricted and subsequently shrinkage occurs. However, cell rupture and deterioration of foam occurs if elasticity is too low at foaming temperature. Another factor is crystallinity. The range of suitable foaming temperatures for crystalline polymers is low. Below melting temperature foaming is not possible and in the molten state appropriate melt strength can only be provided in a small range of temperatures. To overcome this problem, polymers have to be modified in such a way that foamability leads to satisfying results for a wider range of temperatures. Several studies related to the modification of melt strength have been done in the past.[46-48] Recently, Corre et al[46] extended the side chains of crystalline poly(lactic acid) using epoxy additives in a reactive extrusion process before foaming the synthesized material in the presence of supercritical carbon dioxide. They could successfully decrease the cell sizes of foams from macro to micro scale. Pilla et al[47] used talc as additive beside epoxy- functionalized chain extender

which caused a more uniform cell structure. A detailed study on the influence of particles on rheological properties and foamability was done by Riahinezhad et al.[49] They investigated the influence of nanoclay on foamability of a homopolymer and blends. Further studies have shown that the use of nanoclay can also reduce bubble coalescence during foaming.[50-51]

1.6. Objective of the present work

Several methods of foaming plastic material were proposed in the previous sections. The aim of this dissertation is the experimental investigation of foams blown with supercritical carbon dioxide in terms of cell sizes and cell densities with a strong focus on controlling rheological properties of the test systems. Two different strategies were chosen in this work. Firstly, non-homogeneity and consequently local differences in elasticity of polymer blends were created by using cross-linked polymer networks which caused harder and softer domains in the polymer matrices. Secondly, immiscible, binary blends were prepared to generate the aforementioned non-homogeneity. The general idea of research is to create a so called “Sea- an- island morphology” on microscopic scale which is displayed schematically in Figure 1.4. Systems having this morphology are characterized by differences in elasticity between matrix and dispersed phase. These differences can be exploited during foaming in terms of modifying cell size, bimodality and content of open cells. The contents of each chapter are explained in the following:

In chapter 2, the concept of Semi- Interpenetrating Polymer Networks (Semi-IPN) was applied to create local differences in elasticity. Polystyrene and methyl methacryclate were polymerized and cross-linked in a polylactic acid (PLA) matrix. The interwoven networks had a locally higher elasticity than the matrix. The resulting foams had smaller cell sizes and higher cell densities than foams of PLA homopolymer; moreover, the cross-linked networks worked as stabilizers during foaming and bubbles nucleated from pure PLA ruptured during growth. Thus, porous biofoams were synthesized.

The concept of Semi- IPN as device for controlling foam morphology was

extended in chapter 3. An In-Situ process was applied to polymerize and foam a liquid mixture of methyl methacrylate monomers containing dissolved polystyrene. The formation of bimodal foam structures was observed for different depressurization rates, initial monomer concentrations, and cross-linking agent concentrations. It was shown that local differences in elasticity between polystyrene matrix and cross-linked polymethyl methacrylate (PMMA) delayed bubble nucleation in cross-linked PMMA which created bimodality in cell sizes.

The non-homogeneity of polymer blends presented in chapter 4 was created by melt mixing of polystyrene with different types of polyethylene such as high density polyethylene (HDPE), high melt strength polyethylene (HMS-PE), and linear low density polyethylene (LLDPE). It was shown that small amounts of polyethylene can induce heterogeneous nucleation and work as cell opening agents at elevated temperatures over melting temperature of polyethylene. Moreover, it was found that expandability of bubbles correlates with absolute value of complex viscosity.

A summary of the experimental work is given in chapter 5.

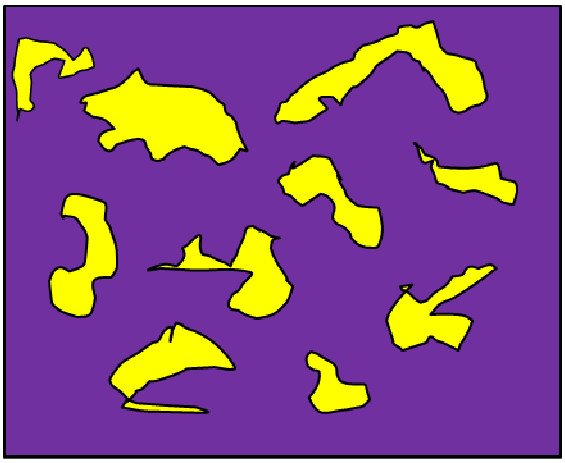

Figure 1.4. “Sea- and- island morphology” of a polymer blend consisting either of immiscible or partly miscible polymers. The bright, yellow domains portray the dispersed component surrounded by the dark, purple polymer matrix.

1.7. References

[1] T. A. Osswald, G. Menges, *Materials Science of Polymers for Engineers*, 2nd edition, Hanser Publishers, Munich 2003, p. 3.

[2] D. Klempner, K. C. Frisch, *Polymeric Foams*, Hanser Publishers, Munich 1991, preface

[3] T. A. Osswald, G. Menges, *Materials Science of Polymers for Engineers*, 2nd edition, Hanser Publishers, Munich 2003, p. 233.

[4] R. T. Fenner, *Principles of Polymer Processing*, The Macmillan Press Ltd., London and Basingstoke 1979, p. 15.

[5] S. L. Rosen, *Fundamental Principles of Polymeric Materials*, John Wiley & Sons Inc., New York 1982, p. 296- 297.

[6] Z. Tadmor, C. G. Gogos, *Principles of Polymer Processing*, John Wiley & Sons Inc., New York 1979, p. 16.

[7] S. L. Rosen, *Fundamental Principles of Polymeric Materials*, John Wiley & Sons Inc., New York 1982, p. 288- 290.

[8] R. T. Fenner, *Principles of Polymer Processing*, The Macmillan Press Ltd., London and Basingstoke 1979, p. 13.

[9] D. Klempner, K. C. Frisch, *Polymeric Foams*, Hanser Publishers, Munich 1991, p. 135- 137.

[10] D. Klempner, K. C. Frisch, *Polymeric Foams*, Hanser Publishers, Munich 1991, p. 197-198.

[11] R. Vieweg, K. Krekeler, *Kunststoff- Handbuch Band 1- Grundlagen*, Carl Hanser Verlag, Munich 1975, p. 1130. *(German version)*

[12] D. Klempner, K. C. Frisch, *Polymeric Foams*, Hanser Publishers, Munich 1991, p.

1.

[13] D. Klempner, K. C. Frisch, *Polymeric Foams*, Hanser Publishers, Munich 1991, p. 379.

[14] D. Klempner, K. C. Frisch, *Polymeric Foams*, Hanser Publishers, Munich 1991, p. 382.

[15] S. S. Yelisetty, D. P. Visco, *J. Chem. Eng. Data* **2009**, *54*, 781.

[16] A. H. Behravesh, C. B. Park, L. K. Cheung, R. D. Venter, *J. Vinyl Addit. Tech.* **1996**, *2*, 349.

[17] D. Miller, V. Kumar, *Polymer* **2011**, *52*, 2910.

[18] T. Otsuka, K. Taki, M. Ohshima, *Macromol. Mater. Eng.* **2008**, *293*, 78.

[19] K. Taki, Y. Warantani, M. Ohshima, *Macromol. Mater. Eng.* **2008**, *293*, 589.

[20] J. A. Reglero Ruiz, J. Marc-Tallon, M. Pedros, M. Dumon, *J. Supercrit. Fluid* **2011**, *57*, 87.

[21] JP 2007291233-A (2007), MITSUI CHEM INC (MITA-C), invs.: N. Inoue.

[22] D. F. Baldwin, C. B. Park, N. P. Suh, *Polym. Eng. Sci* **1996**, *36*, 1437.

[23] D. F. Baldwin, C. B. Park, N. P. Suh, *Polym. Eng. Sci* **1996**, *36*, 1446.

[24] N. H. Abu-Zahra, A. M. Alian, R. Perez and H. Chang, *J. Reinf. Plast. Comp.* **2010**, *29*, 1153.

[25] A. K. Mohanty, M. Misra, G. Hinrichsen, *Macromol. Mater Eng.* **2000**, *276-277*, 1.

[26] S. P. Wu, J. F. Qiu, M. Z. Rong, M. Q. Zhang, L. Y. Zhang, *Polym Int* **2009**, *58*, 403.

[27] J.-D. Mathias, N. Tessier-Doyen, P. Michaud, *Int. J. Mol. Sci.* **2011**, *12*, 1175.

[28] J. S. Chiou, J. W. Barlow, D. R. Paul, *J. Appl. Polym. Sci.* **1985**, *30***,** 2633.

[29] G. K. Fleming, W. J. Koros, *Macromolecules* **1986,** *19***,** 2285.

[30] A. R. Berens, G. S. Huvard, R. W. Korsmeyer, F. W. Kunig, *J. Appl. Polym. Sci.* **1992,** *46***,** 231.

[31] V. Kumar, J. E. Weller, *J. Eng. Ind.* **1994**, *116*, 413.

[32] W. L Zhu, M. Y. Wang, S. N. Leung, C. B. Park, J. Randall, ANTEC 2010, Orlando, Florida USA, May 16-20.

[33] P. C. Lee, J. Wang, C. B. Park, *Ind. Eng. Chem. Res.* **2006**, *45*, 175.

[34] C. B. Park, V. Padareva, P. C. Lee, H. E. Naguib, *J. Polym. Eng.* **2005**, *25*, 239.

[35] H. Ruckdäschel, P. Gutmann, V. Altstädt, H. Schmalz, A. H. E. Müller, *Adv. Polym. Sci.* **2010**, *227*, 199.

[36] H.- G. Elias, *Macromolecules Vol.4: Applications of Polymers*, Wiley-VCH Verlag GmbH & Co. KGaA, Weinheim 2009, p. 416.

[37] H.- G. Elias, *Macromolecules Vol.3: Physical Structures and Properties*, Wiley-VCH Verlag GmbH & Co. KGaA, Weinheim 2008, p. 308.

[38] H.- G. Elias, *Macromolecules Vol.4: Applications of Polymers*, Wiley-VCH Verlag GmbH & Co. KGaA, Weinheim 2009, p. 418.

[39] H.- G. Elias, *Macromolecules Vol.3: Physical Structures and Properties*, Wiley-VCH Verlag GmbH & Co. KGaA, Weinheim 2008, p. 309.

[40] H.- G. Elias, *Macromolecules Vol.3: Physical Structures and Properties*, Wiley-VCH Verlag GmbH & Co. KGaA, Weinheim 2008, p. 312.

[41] H.- G. Elias, *Macromolecules Vol.3: Physical Structures and Properties*, Wiley-VCH Verlag GmbH & Co. KGaA, Weinheim 2008, p. 320.

[42] H.- G. Elias, *Macromolecules Vol.4: Applications of Polymers*, Wiley-VCH Verlag GmbH & Co. KGaA, Weinheim 2009, p. 419.

[43] H.- G. Elias, *Macromolecules Vol.4: Applications of Polymers*, Wiley-VCH Verlag

GmbH & Co. KGaA, Weinheim 2009, p. 420.

[44] R. Liao, W. Yu, C. Zhou, *Polymer* **2010**, *51*, 568.

[45] R. Liao, W. Yu, C. Zhou, *Polymer* **2010**, *51*, 6334.

[46] Y.- M. Corre, A. Maazouz, J. Duchet, J. Reignier, *J. Supercrit. Fluids* **2011**, *58*, 177.

[47] S. Pilla, S. G. Kim, G. K. Auer, S. Gong, C. B. Park, *Polym. Eng. Sci.* **2009**, *49*, 1653.

[48] S. Pilla, A. Kramschuster, L. Yang, J. Lee, S. Gong, L.- S. Turng, *Mater. Sci. Eng. C* **2009**, *29*, 1258.

[49] M. Riahinezhad, I. Ghasemi, M. Karrabi, H. Azizi, *Polym. Comp.* **2010**, *31*, 1808.

[50] M. Mitsunaga, Y. Ito, S. S. Ray, M. Okamoto, K. Hironaka, *Macromol. Mater. Eng.* **2003**, *288*, 543.

[51] Z. R. Xu, H. Y. Park, H. Y. Kim, K. H. Seo, *Macromol. Symp.* **2008**, *264*, 18.

Chapter 2

Open Cell Microcellular Foams of Polylactic Acid (PLA) based Blends with Semi-Interpenetrating Polymer Networks

2.1. Introduction

Porous materials have specific properties, such as high surface area, high permeability, lightweight, and low thermal conductivity. Because of these characteristics, a wide range of applications have been researched and advanced for catalyst supports, membranes, filters, bioscaffolds, porous electrodes, lightweight materials, and insulators. There are several techniques for fabricating polymeric porous structures: porogen leaching, microbead patterning, phase separation, drying of polymer blend solution, gas foaming, 3D printing, and freeze/freeze-drying. Among them, foaming is the simplest and most commonly used production method to prepare polymeric porous materials. Due to the environmentally benign material production, foams of green polymers such as polylactic acid (PLA) and its copolymers with carbon dioxide or nitrogen are very promising for the foaming industry.[1]

Any porous materials have to fulfill certain requirements, such as cell size and cell density, depending upon the application. For bio-scaffold as well as acoustic absorption applications, high open cell content (OCC) is required. Several cell opening strategies have already been studied and proposed: making high temperature differences between the surface and core of an extrudate,[2] using mixed blowing agents[3] to induce secondary nucleation and changes in cell densities, interpolymer blending,[4] and

blending of two polymers with different crystallization temperatures.[5] Park et al[6] proposed a concept of preparing open cell extrusion foams from low density polyethylene (LDPE)- polystyrene (PS) blends. They exploited a structural non-homogeneity of the polymer blend, consisting of hard and soft regions, so as to promote cell opening. The soft regions were used to create pores that interconnected cells in the thinning cell walls during cell growth, while the hard regions held the overall cellular structure so that the cells could not completely coalesce with each other. They used a cross-linking agent to form these hard/soft regions in LDPE-PS blends.

In this chapter, we extended their concept to create open cell foam in the wall of a micro-scale cell. To form the hard/soft regions in microcellular wall, we employed an Interpenetrating Polymer Network (IPN) structure.[7] The IPN comprises two or more networks which are at least partially interlaced physically but not chemically bonded to each other. The networks are entangled in a way such that they cannot be pulled apart. The IPN is characterized either by cross-linking of all components in an interwoven state on a molecular level, or by cross-linking of only one component, which is called Semi-IPN. In both IPN and Semi-IPN structures, two components are intertwined and entangled, however, there are still domains (regions) having higher concentrations of one component. We used these domains as a cell opening agent as well as a bubble nucleating agent. We prepared Semi-IPN from amorphous polylactic acid ($P_{L,D}LA$) based blends in which either styrene or methyl methacrylate monomer were impregnated and polymerized in a $P_{L,D}LA$ matrix. A cross-linking agent was used to control rheological properties in such a way that an appropriate foamability could be provided and the cell size could be reduced. In this study, methods for synthesizing and foaming the Semi-IPN were proposed. The effects of impregnated monomers and the

composition of cross-linking agents on cell structure were investigated as well.

2.2. Experimental

2.2.1. Materials

Amorphous polylactic acid ($P_{L,D}LA$, Polymer 4060D, MW: 197K, NatureWorks) was provided as pellets and used as received. Styrene and MMA (Wako Pure Chemical Industries, Ltd.; Japan) monomers were purified by activated alumina powder (Wako Pure Chemical Industries, Ltd.; Japan) for polymerization with cross-linking agent in $P_{L,D}LA$. Chloroform (Wako Pure Chemical Industries, Ltd.; Japan) and 2,2`-Azobis isobutyronitrile (AIBN, Wako Pure Chemical Industries, Ltd.; Japan) were used as the solvent and initiator for polymerization, respectively. Divinylbenzene isomer (DVB, Wako Pure Chemical Industries, Ltd.; Japan) was used as an aromatic cross-linking agent.

2.2.2. Preparation of IPN blends with and without cross-linking

12 g of $P_{L,D}LA$ pellets were immersed in a mixture of 12 g Chloroform, 4 g of liquid monomer (either Styrene or MMA), 0.04 g (1wt.-%) AIBN at four different DVB contents, 0 g, 0.2 g, 0.4 g and 0.6 g (0wt.-%, 5wt.-%, 10wt.-%, or 15wt.-% of monomer). The solution was mixed and stored at 4 °C for at least 12 hours to prepare a homogeneous and highly viscous liquid. During mixing, the temperature was kept at 4 °C to minimize monomer evaporation loss. Then the solution was heated using a hot press machine to evaporate the solvent, polymerize the monomers in $P_{L,D}LA$, and initiate the cross-linking reaction. Three different temperature levels were used during polymerization. To initiate polymerization of the monomers, the temperature was first

set to 90 °C and maintained for 1 hour. Subsequently, the second temperature was 110 °C for 30 minutes and the third was 180 °C for 30 minutes to complete the polymerization. To enhance the overall uniformity of the samples, the prepared blend sample was crushed once and reshaped to a rectangular shaped plate on the hot press for 20 minutes at 110 °C. No specific mechanical pressure was introduced during the reshaping process while keeping the mold space between the two parallel plates at approximately 1 mm.

For comparison, pure $P_{L,D}LA$ without MMA and styrene monomers was prepared in the same way with different concentrations of cross-linking agent. $P_{L,D}LA$ was dissolved into chloroform with a 1:2 polymer-solvent ratio before adding DVB. To investigate the performance of the cross-linking agent on styrene and methyl methacrylate in $P_{L,D}LA$ matrix, polystyrene (PS) and polymethyl methacrylate (PMMA) were also prepared from the same monomer by directly mixing with the cross-linking agent, DVB, (3 wt.-%, 5 wt.-%, 10 wt.-%, and 15 wt.-%) and 1 wt.-% of AIBN.

2.2.3. Rheological properties

To investigate the effect of DVB and monomer concentration on the resulting polymer blends' morphology, the shear storage modulus (G') and shear loss modulus (G'') of the samples were measured before foaming. A rheometer (Rheometric Scientific; Advanced Rheometric Expansion System ARES) equipped with a rectangular torsion geometry was used to conduct dynamic temperature ramp tests starting from 30 °C up to 125 °C at a heating rate of 2 °C·min^{-1}. The constant oscillation frequency of the torsion bar was set to 1 rad·s^{-1} with 0.1% constant strain. The test specimens were prepared to be approximately 11 mm in width, 1 mm in thickness, and 32 mm in length.

2.2.4. Degree of cross-linking

In the Semi-IPN, one of the two polymers was cross-linked and all components are intertwined on a molecular level. As stated in Lumelsky et al,[8] the non-cross-linked polymer can be removed from the semi-IPN system by means of appropriate solvents. This property was used to identify the degree of cross-linking as gel content. The samples were mixed with chloroform at a solvent-polymer ratio of 30:1 to measure the gel content. The gel was obtained after 24 hours leaching at room temperature. Then the gel was dried for an additional 48 hours at 80 °C. Weighing the residual gel and the initial blend sample can determine the gel content by Equation 1:

$$[Gel] = \frac{m_{polymer,end}}{m_{polymer,start}} \cdot 100\% . \quad (1)$$

2.2.5. Foaming of neat $P_{L,D}LA$ and polymer blends

The polymer foams were prepared by a pressure quench batch physical foaming method using CO_2 as a blowing agent. The square samples 1 cm in length and approximately 1 mm in thickness were prepared and put into a 120 cm^3 high pressure autoclave for foaming. After purging the autoclave with 99.9% pure CO_2 (Showa Tansan Japan), the autoclave was heated to 80 °C and pressurized with CO_2. The CO_2 sorption time for all samples was set to 2.5 hours while keeping the temperature and pressure at 80 °C and 10 MPa, respectively. After sorption, the autoclave was depressurized to atmospheric pressure to induce bubble nucleation. The depressurization time for all experiments varied from 32-33 s.

2.2.6. Characterization of foam- expansion ratio and open cell contents

The characterization of foams was conducted by measuring density, porosity, and open cell content (OCC). The density and specific volume of the foam, $V_{specific}$ ($=\rho_{foam}^{-1}$), were measured at room temperature using a Mirage Electronic Densimeter MD-200S, which contains water as a reference fluid. The measurements were conducted more than six times for each sample and the average was taken. The expansion ratio was given by the density ratio of the foamed and the solid samples:

$$\beta = \frac{\rho_{Solid}}{\rho_{Foam}}. \tag{2}$$

Where ρ_{Solid} and ρ_{Foam} are the densities of polymer and its foam at room temperature. The open cell content was determined by comparing the specific volume of the foams, $V_{specific}$ with the actual volume, V_{actual}, of foams measured at room temperature (27 °C) by the gas pycnometer (micromeritics; AccuPyc Ⅱ 1340) with helium as a reference gas. OCC was determined by:

$$OCC = \left(1 - \frac{V_{actual}}{V_{specific}}\right) \cdot 100\%. \tag{3}$$

2.2.7. Characterization of unfoamed and foamed samples

Small amounts of the unfoamed samples after preparation in the mechanical hot press and reshaping were cut in thin samples via a RMC cryomicrotome made by Boekeler and stained in OsO_4 before an investigation of blend structure via tunnel electron microcopy (TEM, JEOL JEM-2000FX) took place.

The cell structure of foams was observed using a scanning electron microscope (SEM, Tiny-SEM 1540 upgraded for higher magnification, Technex Co. Ltd., Japan). The obtained micrographs were analyzed by the image processing software Image J. The cell density (N_f) was calculated by:

$$N_f = \beta \cdot \left(\frac{n}{A} \right)^{1.5} . \qquad (4)$$

where, n is the number of bubbles detected in the area A (in mm^2) of each micrograph, and β is the expansion ratio.

2.3. Results and Discussion

Figure 2.1 shows the gel contents of the PS, PMMA and $P_{L,D}LA$ samples. With the increase of DVB, the gel content increased, i.e., the degree of cross-linking of PS and PMMA increased. Adding only 3 wt.-% of cross-linking agent to methyl metacrylate and styrene provides a gel content over 80 wt.-% for PS and PMMA. In contrast, polylactic acid alone was not cross-linked by DVB although it was dissolved homogeneously in the solvent. It can be assumed that DVB did not re-activate $P_{L,D}LA$ and that the blends of $P_{L,D}LA$-PMMA and $P_{L,D}LA$-PS formed Semi-Interpenetrating

Polymer Networks, which consist of interwoven polylactic acid molecules and three dimensionally cross-linked polystyrene or PMMA molecules. However, judging from the fact that 15% DVB could not achieve 100% gel content, it was highly possible that low molecular weight PMMA and PS existed in the IPNs.

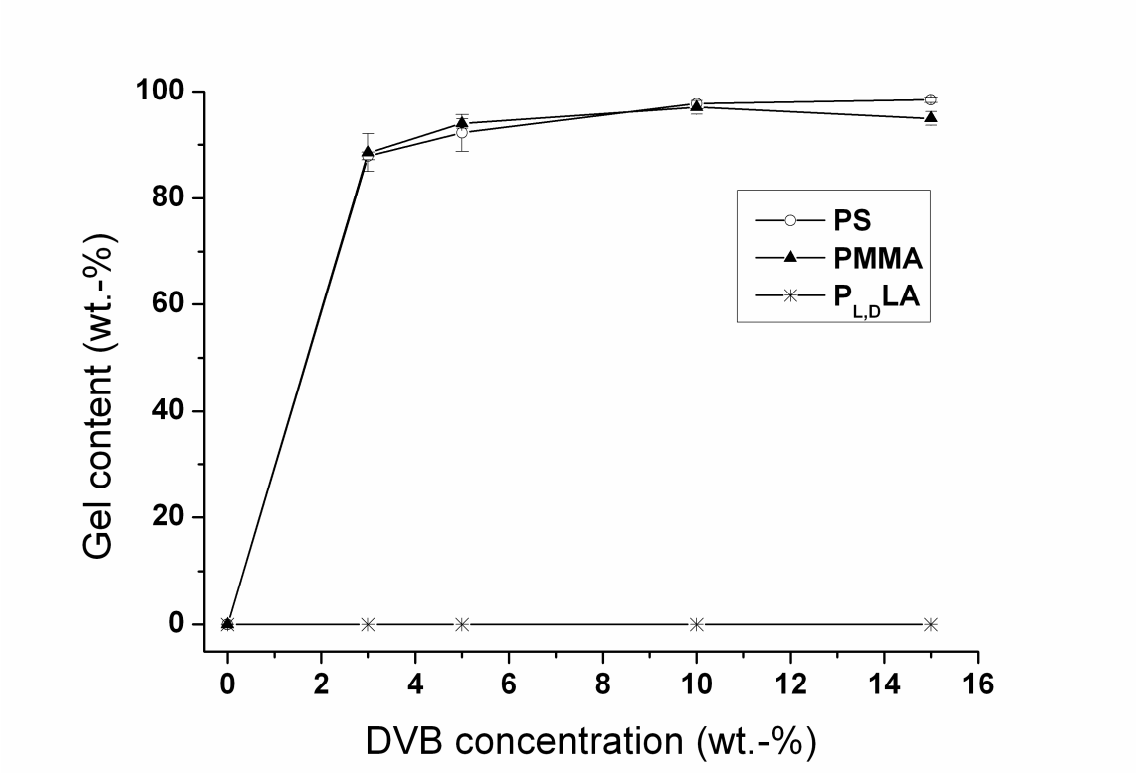

Figure 2.1. Gel content of PS, PMMA, and $P_{L,D}LA$ samples.

2.3.1. Visual observation of unfoamed samples

TEM techniques were applied to investigate samples` micro/ nano structures and to characterize non- homogeneity. Figures 2.2. and 2.3. show the morphology of $P_{L,D}LA$-PS and $P_{L,D}LA$-PMMA blends prepared at 75 to 25 polymer- monomer ratio containing different concentrations of DVB. $P_{L,D}LA$-PS have a distinctive sea- and-island morphology with dispersed polystyrene domains in the $P_{L,D}LA$ matrix as depicted

in Figure 2.2. As DVB concentration is increased up to 15 wt.-%, domain sizes become smaller. Elias[9] mentioned that immiscible polymer blends having positive Gibbs energies of mixing do not demix under certain circumstances, namely if demixing is delayed or kinetically prevented. Thus, a higher degree of cross-linking caused by higher concentrations of DVB prevents formation of bigger domains. The $P_{L,D}$LA-PMMA systems displayed in Figure 2.3. do not show a distinctive reduction of domain sizes; however, the higher the DVB concentration the more distinctive sea- and-island morphology become. $P_{L,D}$LA-PMMA without addition of DVB (Fig. 2.3-a) do not have visible PMMA domains. Possibly, a lack of contrast between matrix and dispersed phase causes “homogeneity”. A more detailed explanation will be given in the rheological section 2.3.2.

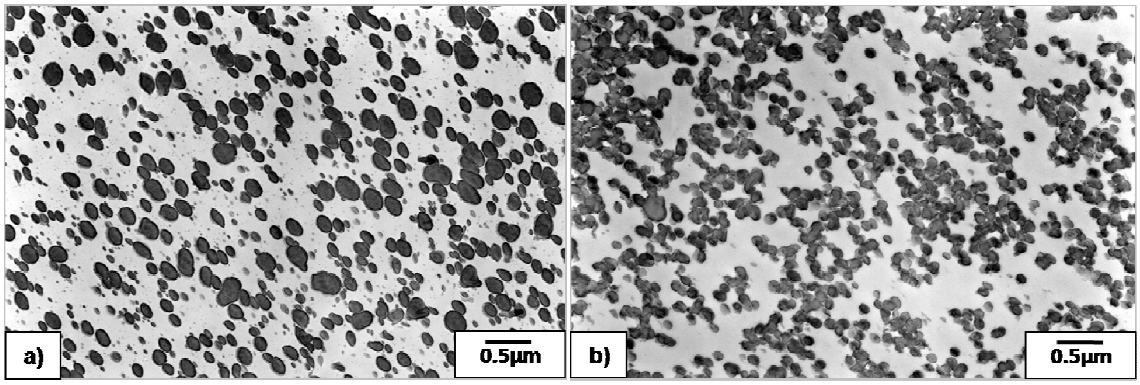

Figure 2.2. TEM micrographs of unfoamed $P_{L,D}$LA-PS (75/25) a) without DVB and b) with 15 wt.-% DVB.

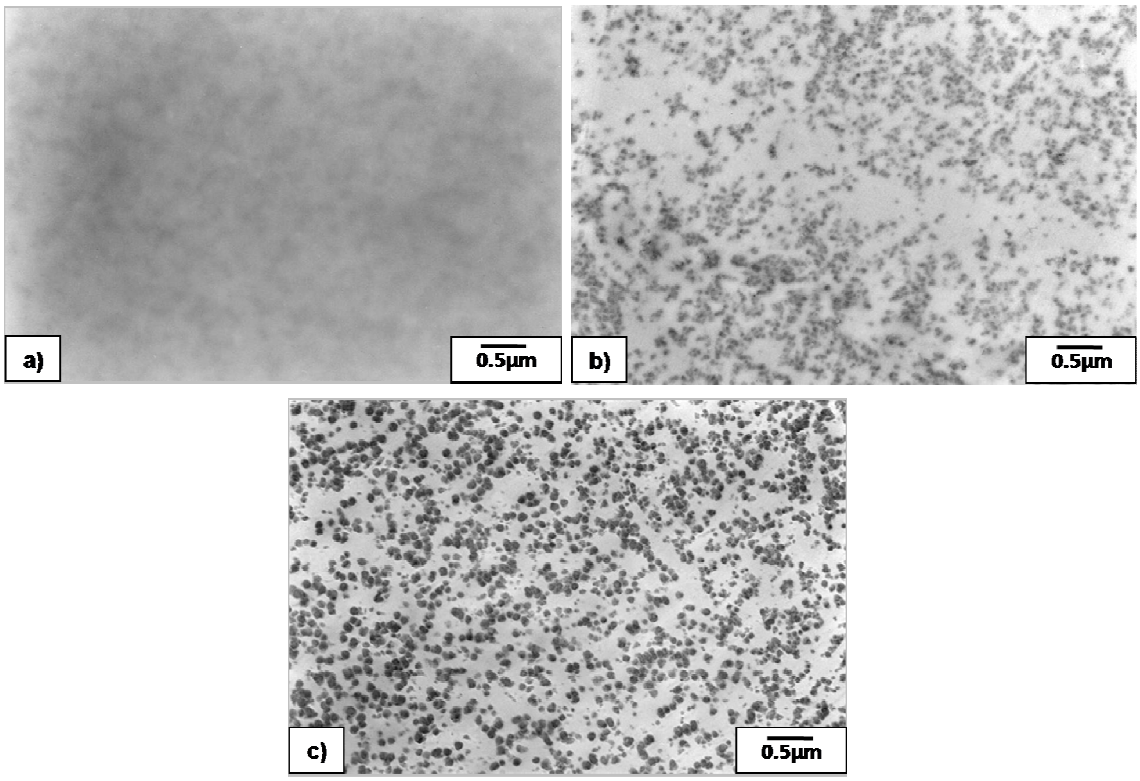

Figure 2.3. TEM micrographs of unfoamed $P_{L,D}LA$-PMMA (75/25) a) without DVB, b) with 5 wt.-% DVB, and c) with 15 wt.-% DVB.

2.3.2. Rheological characterization of synthesized samples

Figure 2.4 shows the storage modulus of neat $P_{L,D}LA$ and $P_{L,D}LA$-PS blends prepared at a 75 to 25 ratio of polymer to monomer with different DVB compositions. In the temperature range from 50 to 120 °C, the storage modulus, G', increased with an increase in DVB content. The increase in G' was observed when the DVB content and monomer concentration were increased in both $P_{L,D}LA$-PS and $P_{L,D}LA$-PMMA systems.

Figure 2.5 shows the relationship of G', measured at 80 °C, to monomer

concentration and DVB content. As shown in Figure 2.5, the increase in monomer and cross-linking agent DVB concentrations increases the storage modulus of the polymer blends. The increase in monomer and cross-linking compositions increases the degree of entanglement and causes higher elasticity of the blend by IPN.

Figure 2.6 shows the loss moduli, G'', of $P_{L,D}LA$ alone, $P_{L,D}LA$-PS, and $P_{L,D}LA$-PMMA blends with different monomer and DVB concentrations. From the curves of loss modulus, G'', versus temperature, the glass transition temperature, T_g, can be identified by the temperature at which G'' reached the maximum.[10-12] T_g increased with an increase in DVB content only for $P_{L,D}LA$-PS systems as illustrated in Figure 2.6-d. The increase in T_g indicates the partial miscibility of polymerized monomers within the $P_{L,D}LA$ matrix. However, it decreased with an increase in DVB concentration in the $P_{L,D}LA$-PMMA (Figure 2.6-c). T_g also decreased with increasing monomer concentration for both blends as illustrated in Figure 2.6-a and 2.6-b. This trend was induced by the plasticization effect of low molecular-weight polymers in the blends. Nielsen[13] described two different effects of cross-linking on T_g: One is the real cross linking effect that was caused by a three dimensional network structure. The effect could lower material's plasticity and increase T_g. The other is the effect of copolymerization of a cross linking agent, which produces a low molecular-weight polymer, and lowers T_g. Steric configuration and chemical structure of the cross-linking agent are crucial for T_g behavior. The peak profile of G" for pure $P_{L,D}LA$ was narrow and distinctive. It became broader as monomers were blended and polymerized. This also indicates the partial miscibility of the blend system.[14] The partial miscibility of the blend with the IPN system can be considered as the polymer chains of both components being intertwined; however, there are still domains having higher concentrations of one

component as illustrated in Figure 2.7-b.[15] The broadness of G" peak profiles were not changed by the concentrations of DVB (Figure 2.6-c and 2.6-d) even though domain sizes change slightly with increasing DVB concentration as depicted in Figure 2.2. Moreover, $P_{L,D}$LA-PMMA sample in Figure 2.3-a) does not have a visible sea- and-island morphology but rheological results in Fig. 2.6-c) indicate non- homogeneity.

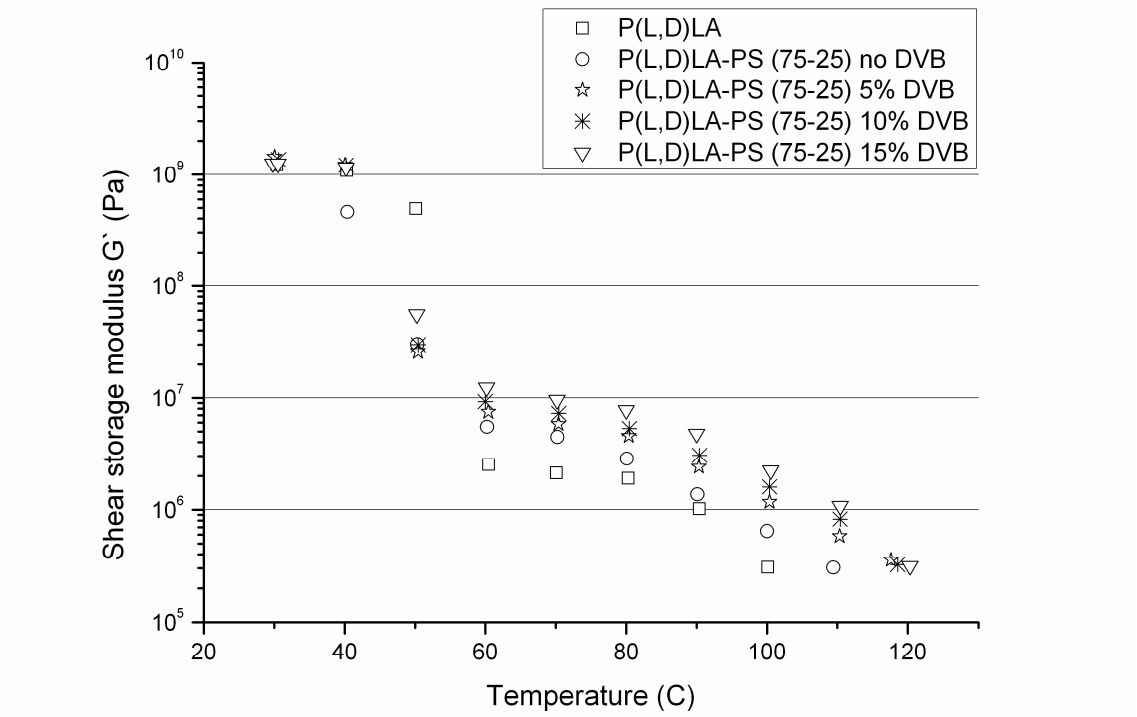

Figure 2.4. Measurements of shear storage moduli G'of $P_{L,D}$LA and $P_{L,D}$LA-PS systems with different DVB concentrations (1 rad·s^{-1} at 0.1% of constant strain).

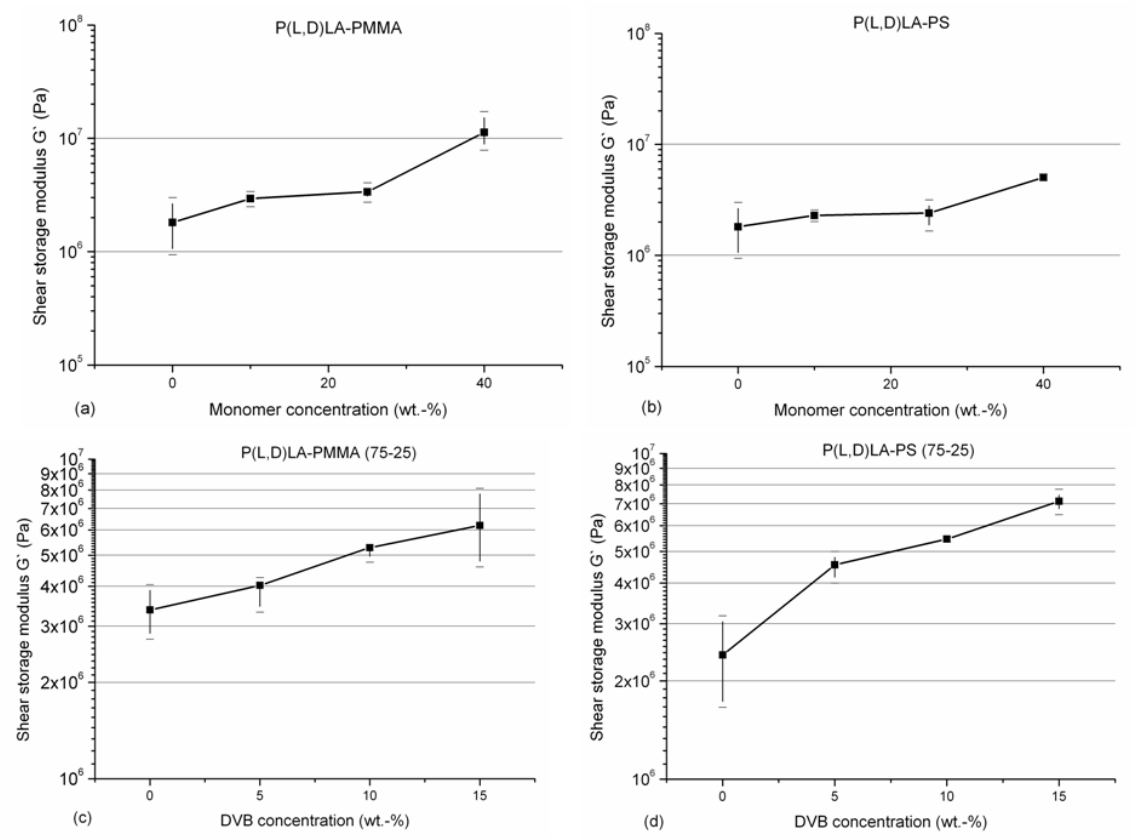

Figure 2.5. Effect of monomer and DVB concentration on the elasticity measured at 80 °C (foaming temperature, at 1 rad·s^{-1} with 0.1% of constant strain). a) and b) blends without DVB, c) and d) blends at 75/25 of $P_{L,D}LA$/monomer ratio.

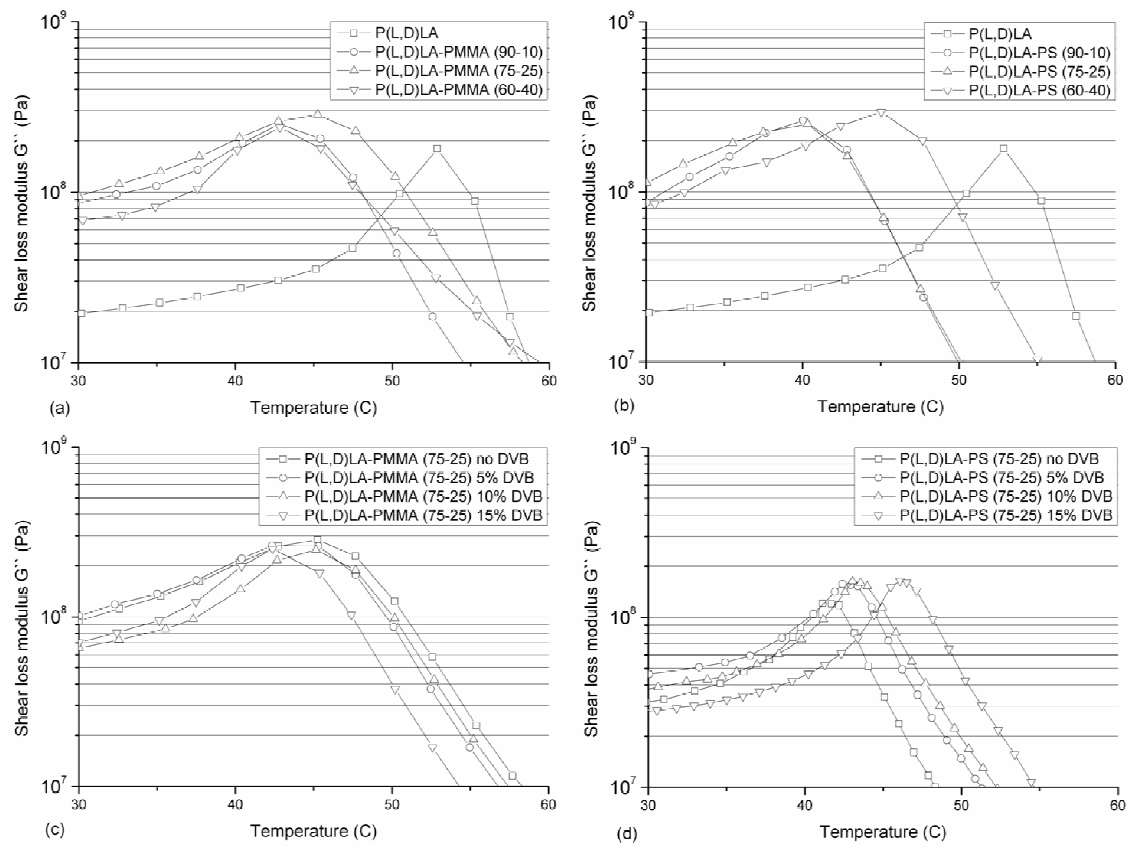

Figure 2.6. Shear loss moduli G'' of investigated systems for different monomer and DVB concentrations. a) $P_{L,D}$LA-PMMA with different polymer/monomer ratios, b) $P_{L,D}$LA-PS with different polymer/monomer ratios, c) $P_{L,D}$LA-PMMA at 75/25 of polymer/monomer ratio with different DVB concentrations, d) $P_{L,D}$LA-PS with a 75/25 polymer/monomer ratio with different DVB concentrations.

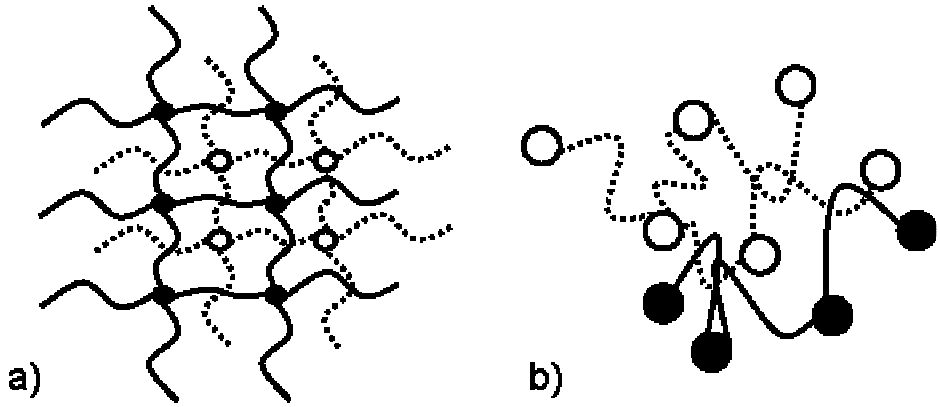

Figure 2.7. Structure of Interpenetrating Polymer Network. a) Homogeneously interwoven IPN. b) Partly miscible IPN.

2.3.3. Expansion ratio

Figure 2.8 shows the expansion ratios of the blend foams prepared with different monomer and DVB compositions. The expansion ratio was reduced by increasing either monomer or DVB concentration. These results underline the fact that the storage moduli, G', was increased at a foaming temperature of 80 ℃ as shown in Figure 2.5. The higher the storage modulus is, the lower expansion becomes.

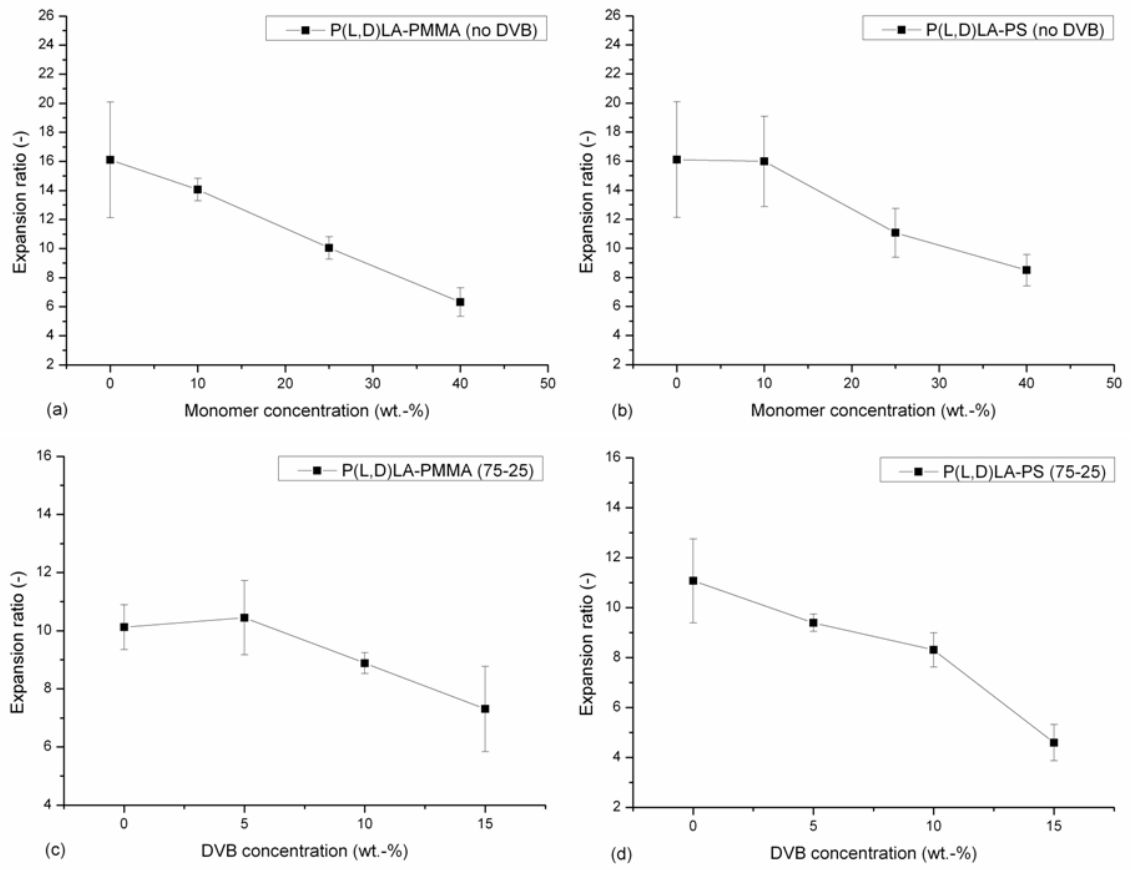

Figure 2.8. Expansion ratios of the foams. a) and b) effect of monomer concentration c) and d) effect of DVB.

2.3.4. Cell size and cell density of foams

The cross-sectional area of the resulting foams was investigated using SEM. Figure 2.9 shows SEM micrographs of the foamed $P_{L,D}$LA-PS samples prepared with different DVB concentrations. An increase in cross-linking agent reduces cell size as shown in Figure 2.9. When DVB was increased to 15%, the cell structure became inhomogeneous, i.e., non-foamed parts existed.

Cell density and size were determined from the SEM micrograph by image-processing using Image J. Figure 2.10 shows how cell density and cell diameter

were changed by monomer and DVB concentration. In both blend systems, with decreasing cell size, the cell density increases. As shown in Figure 2.4 and 2.5, the elasticity of the blend systems increased at a foaming temperature of 80 °C as either monomer or DVB concentration was increased. Higher elasticity suppressed bubble growth and made the cell size smaller. When the cell growth rate was lower, the amount of CO_2 consumed for growing a bubble became smaller and CO_2 concentration dissolved in polymer blend remained higher. As a consequence, the bubble nucleation rate was higher and cell density increased.

As illustrated in Figures 2.2, 2.3, and by rheology data, the blend with the IPN structure tends to have non-uniform morphology. The partial immiscibility forms an inhomogeneous morphology where the polymer chains of both components are intertwined, but, there exists disperse domains having higher concentrations of one component. The inhomogeneous morphology might enhance heterogeneous nucleation; however, it could heavily contribute to open cell content as explained below.

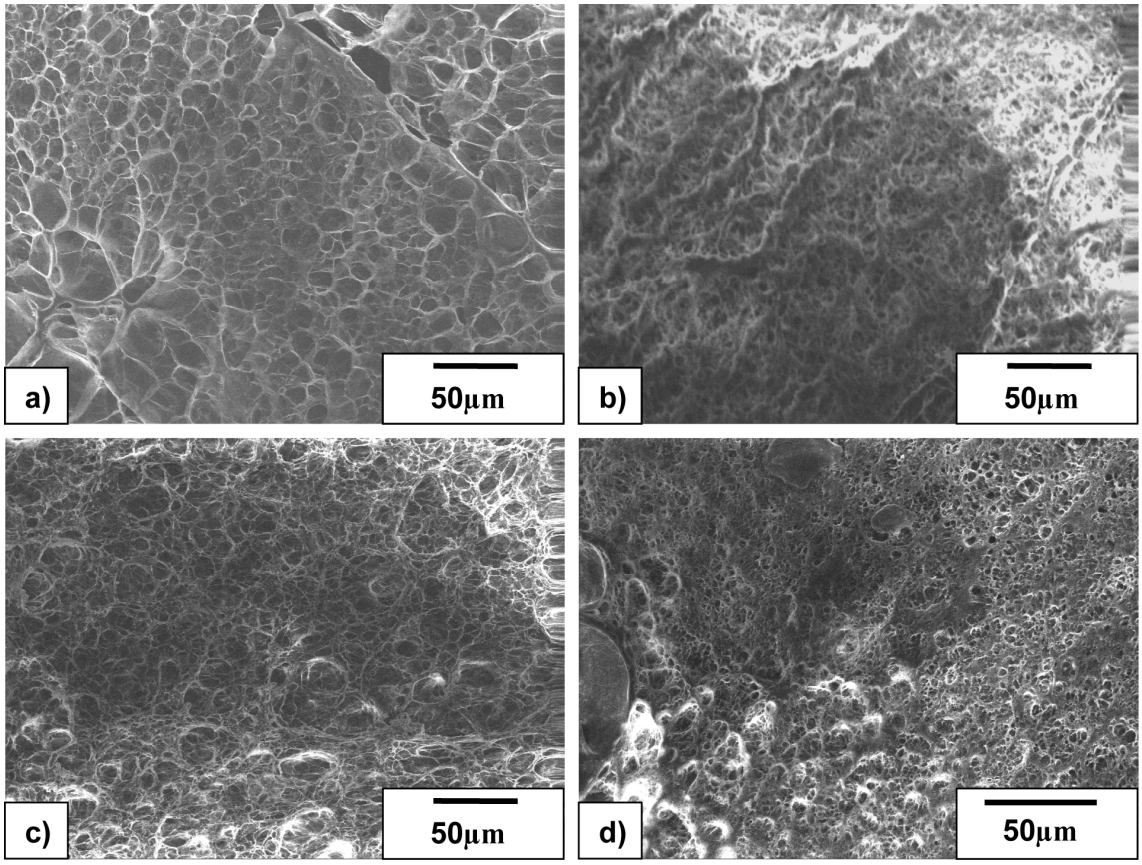

Figure 2.9. SEM images of cross-sectional area of $P_{L,D}LA$-PS foam containing a) no DVB, b) 5 wt.-% DVB, c) 10 wt.-% DVB, d) and 15 wt.-% DVB.

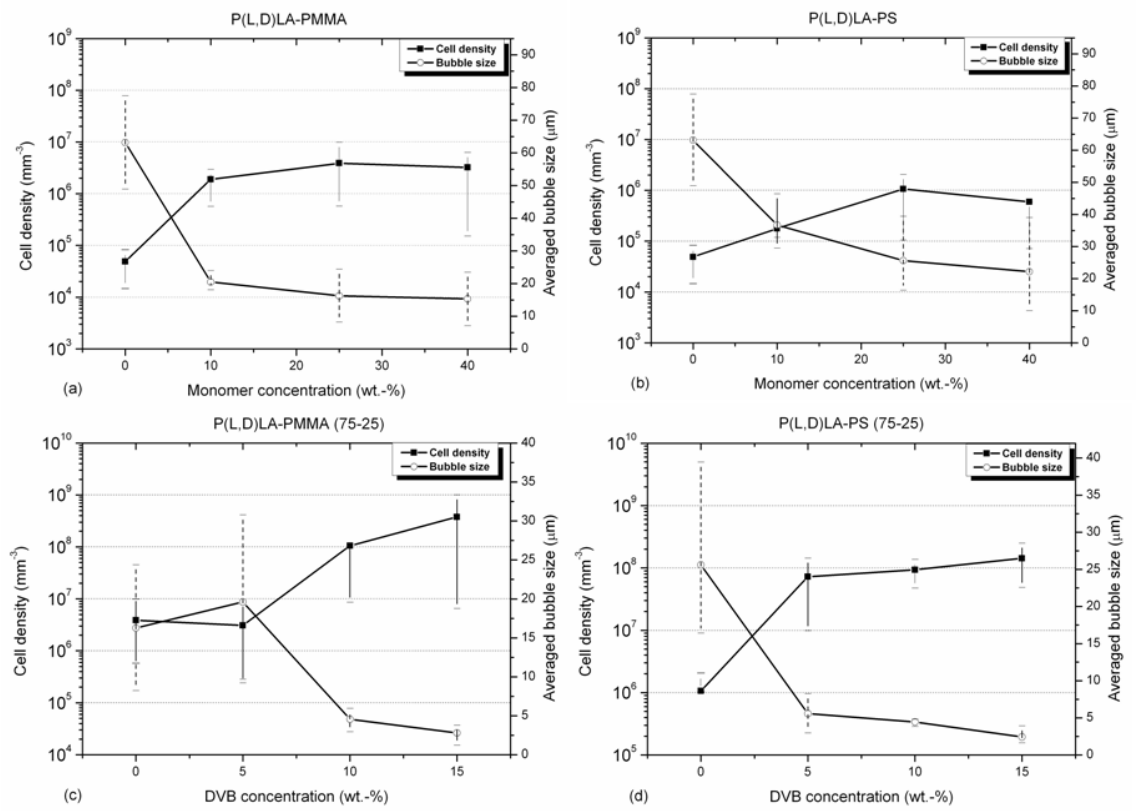

Figure 2.10. Effects of monomer (a, b) and DVB (c, d) concentration on cell density and bubble size in $P_{L,D}LA$-PS and $P_{L,D}LA$-PMMA systems.

2.3.5. Effects of monomer concentration and DVB content on open cell content

The open cell content (OCC) of polymer foams is strongly related to the ability of cell walls to resist rupture during volume expansion. Thus, lower porosity can be expected for polymers with higher elasticity. The higher elasticity at the foaming temperature can make the cell size smaller and prevent rupture.[16] Figure 2.11 shows the OCC of foams prepared with different monomer and DVB compositions. As Figure 2.11-a illustrates, once monomers were mixed and polymerized in $P_{L,D}LA$, the OCC was dramatically increased from that of pure $P_{L,D}LA$ foam. According to Ruckdäschel et al,[17] a cell wall thinning and subsequent rupture is a consequence of the increase of cell

density per volume unit. The displayed cell densities for neat $P_{L,D}LA$ and their blends with 90/10 polymer/monomer ratio in Figures 2.10-a and 2.10-b are in agreement with available literature on cell-opening[17] and with open-cell contents displayed in Figure 2.11-a. A similar tendency is displayed in Figures 2.12-a, -b, and -c. Lower concentrations of monomer reduce cell size, thinning cell walls which originates from higher cell densities, and consequently promote cell wall rupture. However, if the concentration of monomers, i.e. a higher concentration of harder domains, is further increased as depicted in Figure 2.12-c, bubbles can nucleate but their growth is restricted which is indicated by higher cell wall thickness and this consequently leads to a lower OCC. Apparently, the domains having higher concentrations of the polymerized component in the IPN worked as geometric constraint for bubble opening, i.e. the rupture of soft $P_{L,D}LA$ domains surrounded by stabilizing PS or PMMA domains. Fixing initial monomer concentration of either styrene or MMA and increasing degree of cross-linking lowered OCC content continuously (Fig. 2.11-b). The higher degree of cross-linking, the harder PS and PMMA domains became and hindered growth and coalescence of nascent bubbles as exemplarily depicted in Figure 2.9-d. In our case, impregnation and polymerization of styrene and MMA in $P_{L,D}LA$ formed an inhomogeneous morphology. OCC could be controlled by DVB and monomer concentration. Increasing monomer content as well as increasing DVB concentrations made the dynamic shear storage modulus increase and reduced OCC, as shown in Figure 2.11-a and 2.11-b.

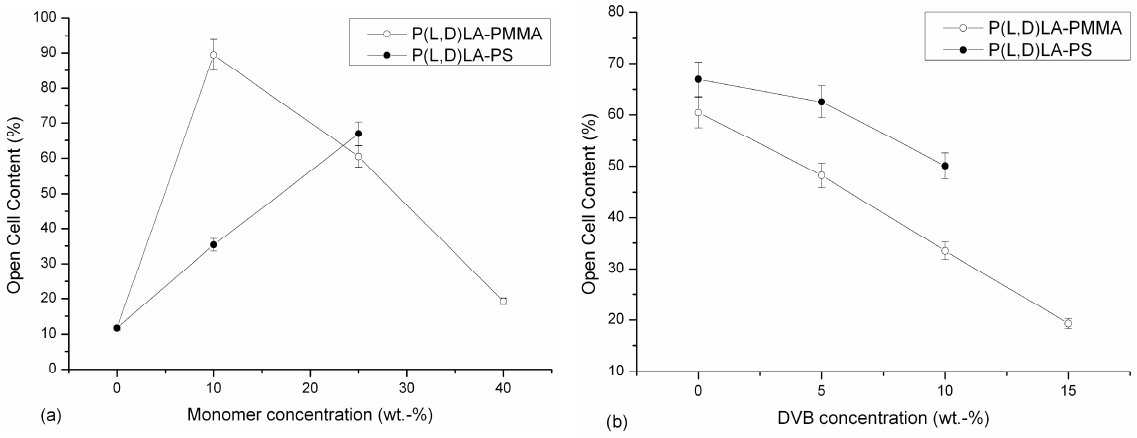

Figure 2.11. a) OCC for systems with different monomer content; b) OCC for different DVB concentrations.

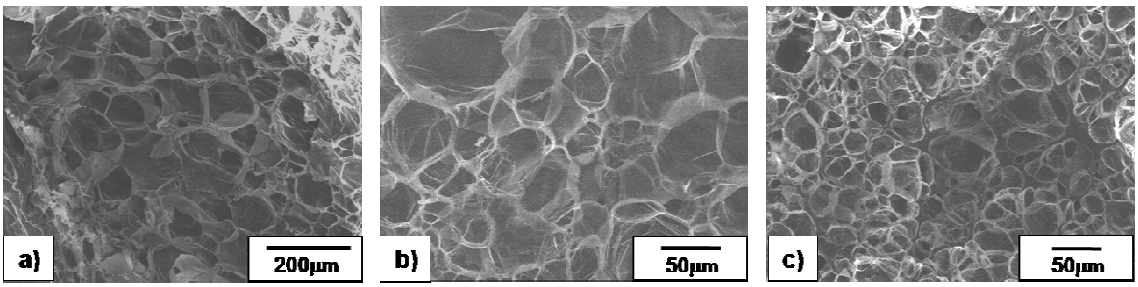

Figure 2.12. Foams of a) neat $P_{L,D}LA$, b) $P_{L,D}LA$-PMMA 90/10, and c) $P_{L,D}LA$-PMMA 60/40.

2.4. Conclusion

Microcellular foams with different open cell content can be prepared using Semi-Interpenetrating Polymer Networks (IPN) on the basis of biodegradable polylactic acid. Different concentrations of divinylbenzene (DVB) cross-linking agent and the initial monomer were used to control viscoelasticity and blend morphology, which changed the averaged bubble size, cell density, and open cell content (OCC) of IPN systems.

2.5. References

[1] Q. Xu, Y. Chang, J. Wang, L. Yu, K. Dean, *J. of Appl. Polym. Sci.* **2004**, *94*, 593.

[2] P. C. Lee, G. Li, J. W. S. Lee, C. B. Park, *J. Cell. Plast.* **2007**, *43*, 431.

[3] P. C. Lee, H. E. Naguib, C. B. Park, J. Wang, *Polym. Eng. Sci.* **2005**, *45*, 1445.

[4] US. 6 174 471 (2001), The Dow Chemical Company MI, invs.: C. P. Park, B. Chaudhary, D. Imeokparia.

[5] P. C. Lee, J. Wang, C. B. Park, *Ind. Eng. Chem. Res.* **2006**, *45*, 175.

[6] C. B. Park, V. Padareva, P. C. Lee, H. E. Naguib, *J. Polym. Eng.* **2005**, *25*, 239.

[7] L. H. Sperling, *J. Polym. Sci., Macromolecular Rev.* **1977**, *12*, 141.

[8] Y. Lumelsky, Z. Zoldan, S. Levenberg, M.S. Silverstein, *Macromolecules* **2008**, *41*, 1469.

[9] H.- G. Elias, *Macromolecules Vol.3: Physical Sturctures and Properties*, Wiley-VCH Verlag GmbH & Co. KGaA, Weinheim 2008, p. 320.

[10] Y. Aoki, *Macromolecules* **1988**, *21*, 1277.

[11] K. Okamoto, T. Ichikawa, T. Yokohara, M. Yamaguchi, *Eur. Polym. J.* **2009**, *45*, 2304.

[12] L. H. Sperling, *Introduction to Physical Polymer Science*, 4st edition, John Wiley & Sons Inc., Hoboken, New Jersey 2006, p. 363.

[13] L. E. Nielsen, *J. Macromol. Sci. Polym. Rev.* **1969**, *3*, 69.

[14] T. Sasaki, T. Uchida, K. Sakurai, *J. Polym. Sci. Polym. Phys.* **2006**, *44*, 1958.

[15] H. Szocik, R. Jantas, *J. Therm. Anal. Calorim.* **2004**, *76*, 307.

[16] W. L. Zhu, M. Y. Wang, S. N. Leung, C. B. Park, J. Randall, ANTEC 2010, Orlando, Florida USA, May 16-20.

[17] H. Ruckdäschel, P. Gutmann, V. Altstädt, H. Schmalz, A. H. E. Müller, *Adv.*

Polym. Sci. **2010**, *227*, 199.

Chapter 3

In-Situ Preparation of Cross-linked PS-PMMA Blend Foams with a Bimodal Cellular Structure

3.1. Introduction

The preparation and characterization of open pore microcellular foams from amorphous polylactic acid ($P_{L,D}LA$) based blends was discussed in chapter 2. Foams consisting of $P_{L,D}LA$-PS and $P_{L,D}LA$-PMMA systems, respectively, had Semi- IPN structures which could successfully modify cell size, cell density, and open cell content (OCC). The difference of viscosity between the polymer matrix and the cross- linked, dispersed PS and PMMA domains were identified as the crucial factor of preparing microcellular foams with different bulk foam densities, expansion ratios, and cell morphologies.

In recent studies, the averaged cell size of foamed systems could further be decreased from microscale to nanoscale[1-5] using environmentally benign blowing agents like CO_2 or N_2 which already were studied [6-8] for preparing microcellular foams. Another issue in foaming technology is how to control the cell morphology, such as an open or closed cell structure as well as mono-modal or bi-modal cell size distribution. For acoustic absorption and filter applications, a high open cell content (OCC) is required and some preparation methods are, e.g., high temperature differences between the surface and core of an extrudate,[9] mixed blowing agents,[10] interpolymer blending,[11] polymer blends with different crystallization temperatures,[12] and

non-homogeneity of polymer blend phase morphology with different elasticity.[13] The basic concept of these methods is the same: during the foaming process, bubble nucleation is induced in two stages. After inducing the first bubble nucleation either by depressurization or a temperature increase, the second bubble nucleation is induced with a certain degree of time lag, creating pores that interconnect cells in the thinning cell walls. The time lag is created by either a solubility difference between two different blowing agents,[10] a local temperature difference,[9] or an elasticity difference between two polymers in non-homogeneity.[13]

Bimodal cell size distribution can be also realized by applying one of those two-stage bubble nucleation schemes while making the elasticity and elongational viscosity of the polymer high enough to prevent the cell walls from interconnecting and coalescing. Arora et al.[14] prepared bimodal cellular foams from neat polystyrene by reducing the pressure in two stages, in which the second stage of the pressure drop induces secondary bubble nucleation. Kaneka Co., Ltd. used water as the second blowing agent together with a water-absorptive polymer to create a bimodal cell size distribution in polystyrene foam,[15] which is considered to be a combination of the polymer blend and the solubility difference methods. Daigneault et al. used the method of similar mixed blowing agents to create a bimodal cell size distribution.[16] The authors used a mixture of CO_2 and 2-Ethyl Hexanol (EH) as blowing agents for foaming polystyrene with a bimodal cell size distribution. They assumed that a 2-EH phase existed in PS and that CO_2 bubbles were nucleated in the 2-EH phase first and then in PS. The CO_2 solubility difference between the EH and PS phases activated the two-step bubble nucleation mechanism. In addition, there are several papers reporting the use of phase morphology non-homogeneity of a semi-crystalline polymer to create a bimodal

cell size distribution. Jacobs et al. prepared cellulose acetate butyrate foams with a bimodal cell size distribution by using the time lag between heterogeneous and homogeneous bubble nucleation in which heterogeneous nucleation occurred at the interface of the crystals and homogeneous nucleation in the amorphous region.[17] Jiang et al. also used the crystalline structure to create bimodality of cell size in PP foam.[18] Xu et al. investigated CO_2 physical foaming of polypropylene and reported that the bimodal cell size distribution could be realized by increasing the sorption pressure and depressurization rate while setting the foaming temperature close to the melting point of PP.[19] The authors mentioned that the increase in the depressurization rate enabled the bubble nucleation in the crystalline region, and the bubbles in the amorphous region grew bigger than those in the crystalline region because the amorphous region was less rigid than the crystalline region. However, the bimodality created by the crystalline nature[17-19] could easily disappear with slight changes in the foaming temperature or depressurization rate.

In this chapter, the non-homogeneity of the polymer blend phase morphology, as well as the elasticity difference between the polymers were exploited to create the bimodal cell size distribution, in which the first bubble nucleation occurs in the less rigid domain and the second in the rigid region. An interpenetrating polymer network (IPN) of a PS and PMMA blend was foamed.[20] The blend was prepared by infusing methyl methacrylate (MMA) monomer into PS and polymerizing MMA in contact with pressurized CO_2. The resulting blend with a Semi-IPN has PS and PMMA networks that are interlaced and entangled on a molecular level. The advantage of non-homogeneity in the blend phase morphology with a local modification of elasticity of the PMMA domains was taken to create the bimodal cell size distribution at moderate

depressurization rates.

3.2. Experimental

3.2.1. Materials

Polystyrene (PS, MW: 192K, Sigma- Aldrich Inc.; USA) was provided as pellets and was used as received. Methyl methacrylate (Wako Pure Chemical Industries, Ltd.; Japan) monomers were purified by activated alumina powder (Wako Pure Chemical Industries, Ltd.; Japan) for polymerization with a cross-linking agent in the PS matrix. An initiator for polymerization, 2,2`-Azobis isobutyronitrile (AIBN, Wako Pure Chemical Industries, Ltd.; Japan), was used, and Diurethane dimethacrylate (DUDMA, mixture of isomers, Sigma-Aldrich, Inc.; USA) was the cross-linking agent.

3.2.2. Preparation of PS/PMMA blends for foaming

Table 3.1 shows the prepared PS/PMMA blends for foaming experiments. Two grams of PS pellets were mixed with either 2 or 4 g of liquid MMA monomers and 1 wt.-% AIBN. Two polymer solutions with different compositions (PS/MMA 50:50, PS/MMA 33:67, or PS/MMA 15:85) were prepared. The amount of AIBN was changed in accordance with the MMA concentrations. The concentration of DUDMA cross-linking agent was changed to 0.5, 2, and 5 wt.-% (0.01, 0.04, and 0.1 g) to investigate the effect of the degree of cross-linking. DUDMA and AIBN were mixed and dissolved with MMA in a closed flask before loading the PS pellets. The PS/MMA solutions were placed in a refrigerator and stored at 4 °C for at least 12 hours to dissolve the PS pellets in the MMA monomer and to obtain a homogeneous, viscous polymer solution. Additional solvent was not needed for preparing the solution because PS

dissolved in the MMA. Subsequently, the resulting single phase mixture was poured into a bowl made of aluminum foil before being placed into an autoclave.

Table 3.1. Preparation condition of PS/MMA systems (O indicates systems prepared for foaming).

Ratio	0.5wt.-% DUDMA	2wt.-% DUDMA	5wt.-% DUDMA
PS/MMA 50:50	◯	◯	◯
PS/MMA 33:67	◯	-	-
PS/MMA 15:85	◯	-	-

3.2.3. Preparation of neat PS and PS/PMMA blends for rheological investigations

To measure the rheological properties of PS/PMMA as well as neat PS, samples were prepared from the same ingredients using pressurized CO_2. Neat PS pellets were heated and shaped into a plate at 120 °C for 20 minutes using a hot press. PS/MMA (50:50) with 0.5 wt.-% DUDMA, PS/MMA (50:50) with 2 wt.-% DUDMA, and PS/MMA (33:67) with 0.5 wt.-% DUDMA were also prepared using the hot press. In-situ polymerization of the PS/MMA mixture was conducted without using CO_2 in the hot press by setting the processing temperature to 100 °C for 4 hours, then increasing the temperature to 120 °C, keeping in the sample in the press for an additional 20 minutes and compressing it slightly to shape the sample into a rectangular plate.

3.2.4. Rheological Properties

To investigate the effects of polymerized MMA in the PS matrix and the DUDMA cross-linking agent on the cell structure of foam, the shear storage modulus (G') and shear loss modulus (G'') were measured. A rheometer (Rheometric Scientific;

Advanced Rheometric Expansion System ARES) equipped with a rectangular torsion geometry was used to conduct dynamic temperature ramp tests from 50 to 180 °C at a heating rate of 2 °C·min^{-1}. The constant oscillation frequency of the torsion was set to 1 rad·s^{-1} with 0.1% constant strain. The test specimens were approximately 10 mm wide, 1 mm thick, and 25 mm long. The presence of CO_2 in polymer enhances the chain mobility of polymer and reduces the viscoelasticity of polymers. G' and G" of the sample in the presence of pressurized CO_2 could not be measured due to the lack of high pressure rheometers. Thus, we assumed here that CO_2 induced viscosity reduction could shift the G'-temperature or G"-temperature curves toward lower temperature in some degree but could not change the shape of the curves (profiles) and orders of the amplitudes of curves. Furthermore, the rheological data were mainly used in this study to investigate the influence of MMA concentration on miscibility and elasticity and the influence of DUDMA on elasticity.

3.2.5. Foaming of PS/PMMA blends

Pressure-quench batch foaming in an autoclave, 120 cm^3 in volume, was conducted using CO_2 as the physical blowing agent. A two-step processing scheme was employed to foam the samples. The first stage was sorption of CO_2 and MMA into PS. The PS/MMA solution was placed in an autoclave, purged with 99.9% pure carbon dioxide (Showa Tansan Japan), and heated up 60 °C before increasing the CO_2 pressure in the autoclave to 8 MPa. Supercritical CO_2 infusion[21] took place at 60 °C for 4 hours. The temperature at this sorption stage was determined so that the polymerization reaction of MMA in the PS matrix could be suppressed and the sorption of CO_2 and MMA into PS could be enhanced. In the second stage, the temperature was increased to

100 °C for an additional 4 hours while keeping the pressure at 8 MPa to polymerize MMA in PS. A needle value was equipped on the effluent gas line of the autocalve and electrically manipulated by a pressure controller to keep the CO_2 pressure inside autocalve during the heating process. Afterwards, the autoclave was depressurized to atmospheric pressure to foam the samples. The time taken for the pressure to drop to 0.1 from 8 MPa was measured for calculating the approximated depressurization rate. Depressurization rates of 0.15, 0.45, and 0.9 $MPa \cdot s^{-1}$ (1.5, 4.5, and 9 $bar \cdot s^{-1}$) were individually tested during foaming. The foaming temperature was determined to be 100 ^oC by conducting preliminary experiments with foaming temperatures of 85, 100, and 110 ^oC. At a temperature over 110 ^oC, the foams showed an open cell structure, as well as severe distortion of the foams. Contrarily, at a temperature below 85 ^oC, the uniformity of cell structure worsened.

3.2.6. Characterization of foam - bulk foam density

The bulk foam density was measured at room temperature using a Mirage Electronic Densimeter MD-200S, which contains water as a reference fluid. The measurements were conducted seven times for each sample, and the average was taken.

3.2.7. Characterization of foam - cell density and cell size

The cell structure was observed using a scanning electron microscope (SEM, Tiny-SEM 1540 upgraded for higher magnification, Technex Co. Ltd., Japan). The obtained micrographs were analyzed by the image processing software Image J. The cell density (N_f) was calculated by:

$$N_f = \left(\frac{n}{A} \right)^{1.5}. \quad (1)$$

Where, n is the number of bubbles detected in the area A (in mm^2) of each micrograph. The prepared foams have bimodal structures, and therefore, the cell densities and cell sizes are discussed individually in the following sections.

3.3. Results and Discussion

3.3.1. Rheological characterization

Dynamic mechanical thermal analysis (DMTA) was conducted in a temperature range from 50 to 180 °C. Figure 3.1 shows the shear storage modulus G' of neat PS and three PS/PMMA blends. Two of the blends were prepared with the same PS and MMA ratio 50:50 but different concentrations of DUDMA. The other blend was prepared with a PS and MMA ratio of 33:67 while keeping the concentration of cross-linking agents at 0.5 wt.-%. The overall storage modulus was increased in a temperature range from 120 to 180 °C by increasing the DUDMA concentration as well as the MMA monomer content. Enhancing the intermolecular entanglement by increasing either the cross-linking agent or monomer concentrations could increase the elasticity, G', of the blends.

However, even when intertwinement of the polymer chains occurs between two polymers with an increase in the degree of cross-linking, it is possible to formulate PMMA-rich domains in the PS matrix due to the immiscibility of PMMA and PS. The existence of such domain could be confirmed by the rheology data. Every curve of shear loss modulus G'' and temperature in Fig. 3.2 shows a single glass transition temperature (T_g) around 90 °C, which is indicated by the maximum of the curve.[22] The peaks in the G"-temperature curve broadened with an increase in the DUDMA and MMA concentrations. The single glass transition indicates that the sample is either a homopolymer, a miscible polymer blend or two polymers with similar T_g. Aoki[23] reported that peak broadening in the G"-temperature curve indicates the partial miscibility of blended polymers. Therefore in our PS/PMMA blends, there exist some domains or clusters in which the PMMA concentration is higher. This partial miscibility

creates non-homogeneity of the polymer blends and can be utilized to induce bubble nucleation in two steps: first in the PS matrix and then in the PMMA-rich domains.

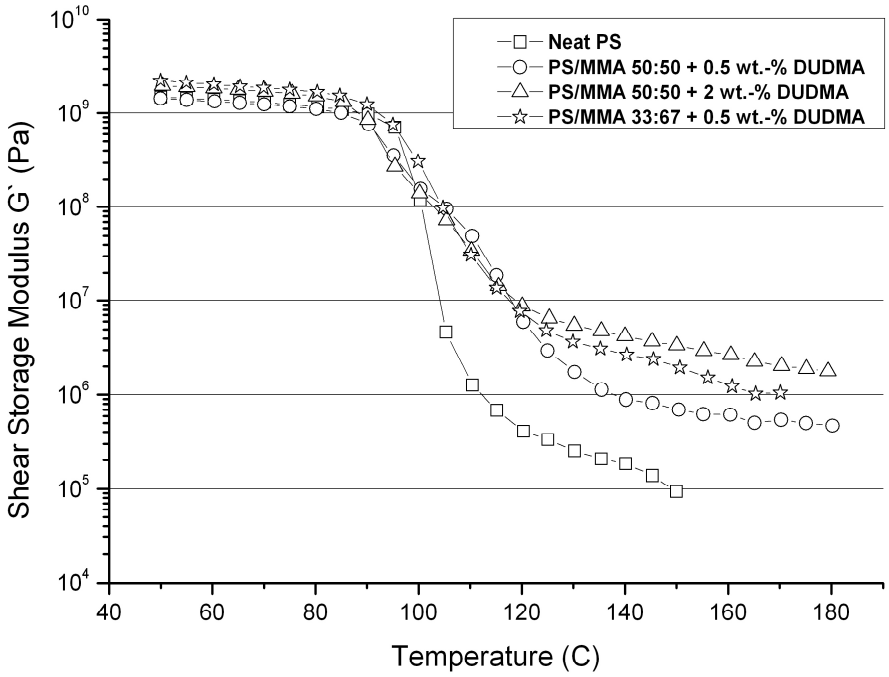

Figure 3.1. Measurements of shear storage moduli G' of neat PS, PS/MMA 50:50 + 0.5 wt.-% DUDMA, PS/MMA 50:50 + 2 wt.-% DUDMA, and PS/MMA 33:67 + 0.5 wt.-% DUDMA (1 rad·s^{-1} at 0.1% of constant strain).

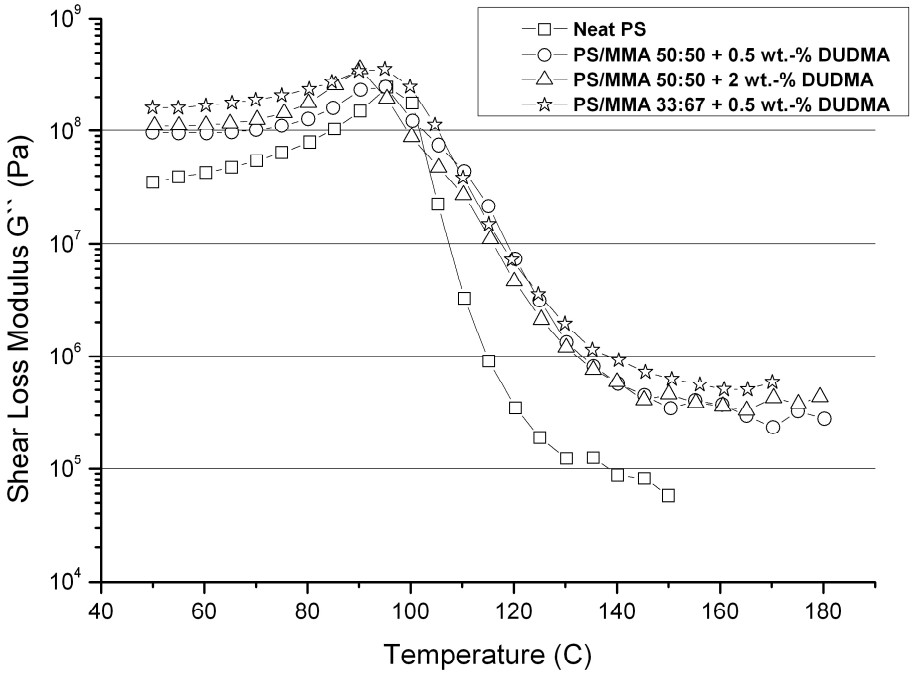

Figure 3.2. Measurements of shear loss moduli G'' of neat PS, PS/MMA 50:50 ＋0.5 wt.-% DUDMA, PS/MMA 50:50 + 2 wt.-% DUDMA, and PS/MMA 33:67 + 0.5 wt.-% DUDMA (1 rad·s^{-1} at 0.1% of constant strain).

3.3.2. Monomer loss during processing

Because MMA can be dissolved in supercritical CO_2, some amount of MMA could not be polymerized but leaked out with CO_2 released for pressure control. This caused a loss of monomer. Thus, the ratio between PS and PMMA in the resulting samples was not equal to the initial ratio of PS and MMA in the loaded solution. The loss of MMA monomer during processing was evaluated by weighing the sample before and after sorption and polymerization. The results are listed in Table 3.2 with standard deviations. For each sample treatment, 20- 30 wt.-% of MMA monomer was lost.

Table 3.2. Average MMA weight loss of the systems during processing.

System	PS/MMA 50:50 + 0.5 wt.-% DUDMA	PS/MMA 50:50 + 2 wt.-% DUDMA	PS/MMA 50:50 + 5 wt.-% DUDMA	PS/MMA 33:67 + 0.5 wt.-% DUDMA
Average weight loss [%]	26.27	27.65	22.16	25.03
Standard deviation [%]	9.45	8.12	5.14	8.38

3.3.3. Effect of depressurization rate

The effect of the depressurization rates on the cell structure was investigated. Depressurization rates, dp/dt, of 1.5, 4.5 and 9 bar·s^{-1} were applied. Figure 3.3 shows SEM micrographs of the cross-sectional area of the foams prepared from PS/MMA (50:50) with three different depressurization rates. The micrographs in the left column show the macroscopic view of the cell structures. Those in the right column are high magnifications of the images on the left and show the microscopic view, especially, the small bubbles in the cell walls of the large bubbles. A bimodal cell structure was successfully formed in every sample. The average diameter of the large bubbles was in the range of 200 - 400 µm, and that of the small bubbles was 10 - 30 µm. The diameters of both the large and small bubbles were not changed drastically by an increase in the depressurization rates as shown in Fig. 3.4. This might be caused by setting the depressurization rate at a lower range. However, the number of small bubbles in the cell

wall increased as the depressurization rate was increased. Figure 3.5 shows the bulk foam density as well as the percentage of the cell wall area where the small bubbles were present, i.e., the percentage of the micro-bubble area. The percentage of the micro-bubble area was calculated from the high-magnification SEM micrograph in the following way: the total area of the cell walls was measured by subtracting the area of large bubbles from the entire area of the SEM image. The areas of the cell wall in which the small bubbles were present were identified and were colored black on the image analyzer. Then, the percentage of the micro-bubble area was calculated by dividing the back area by the total cell wall area. It can be seen that the low depressurization rate made the micro-bubble area less than 10% of the cell walls, whereas the high depressurization rate could increase the percentage to approximately 75%. As can be also seen in Fig. 3.5, the bulk foam density decreased as the percentage of the micro-bubble area increased. It is possible that the increased number of micro-bubbles contributes to the reduction of foam density. Based on the fact that the size of the small bubbles did not change drastically with the depressurization rate, it can be assumed that the micro-bubbles were formed in the PMMA-rich domains in the secondary nucleation process, where the PMMA-rich domain has a higher elasticity than the PS matrix due to cross-linking. The higher elasticity requires a larger driving force to nucleate bubbles in the domain. Thus, the onset of bubble nucleation was delayed in the more elastic domain. The higher depressurization rate, i.e., the larger driving force, could foam the cross-linked PMMA-rich domains.

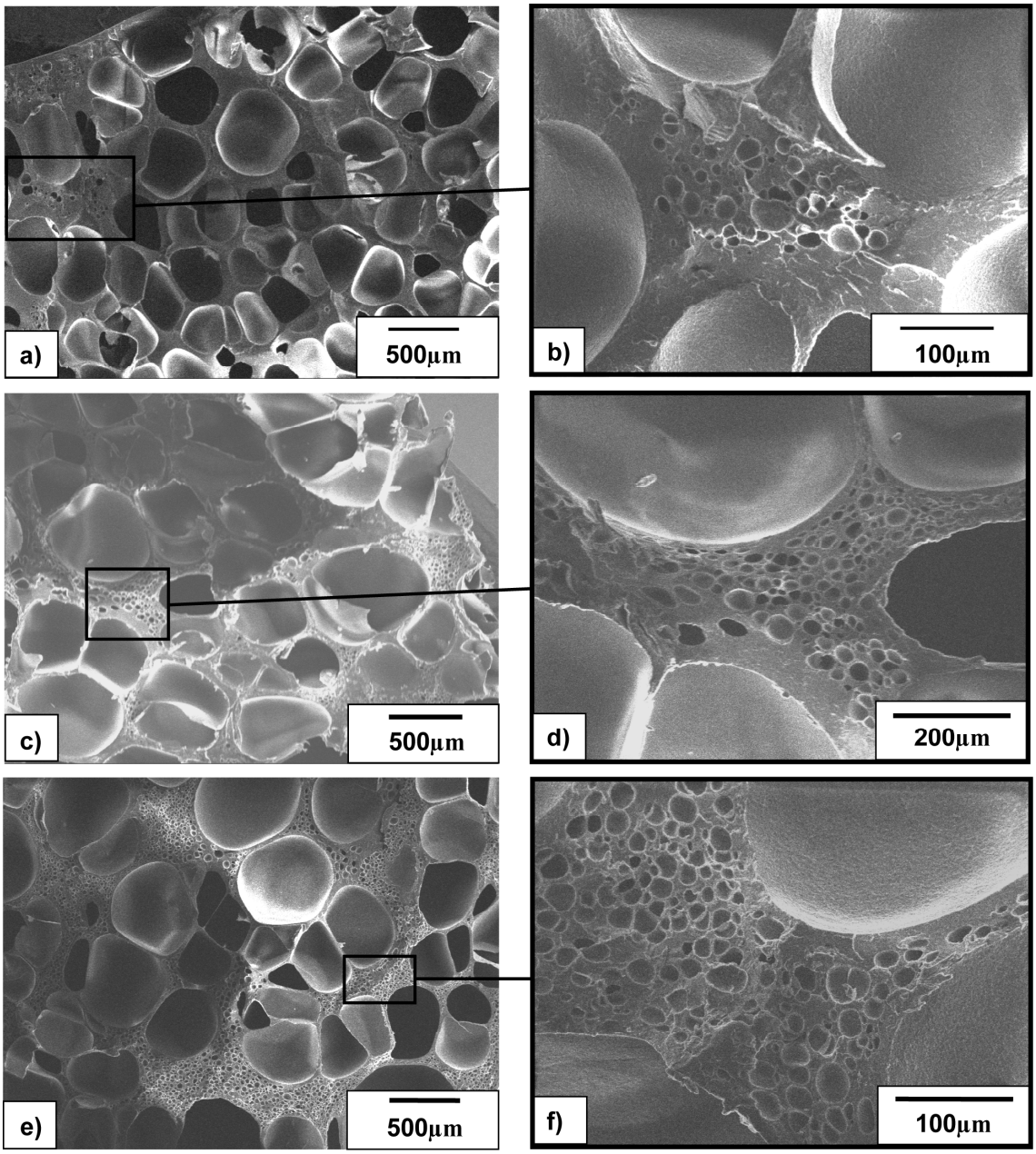

Figure 3.3. Different depressurization rates for the polymer-monomer system, PS/MMA 50:50 + 0.5 wt.-% DUDMA. a) and b): dp/dt= 1.5 bar·s^{-1}; c) and d): dp/dt= 4.5 bar·s^{-1}; e) and f): dp/dt= 9 bar·s^{-1}.

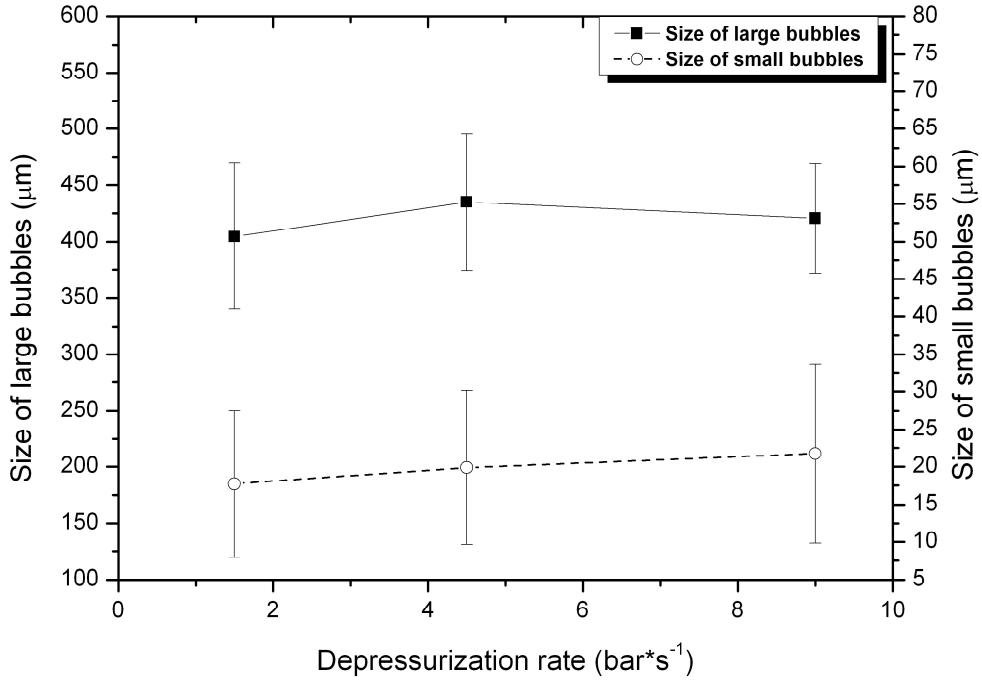

Figure 3.4. Average large and small cell sizes for three different depressurization rates using the PS/MMA 50:50 + 0.5 wt.-% DUDMA system.

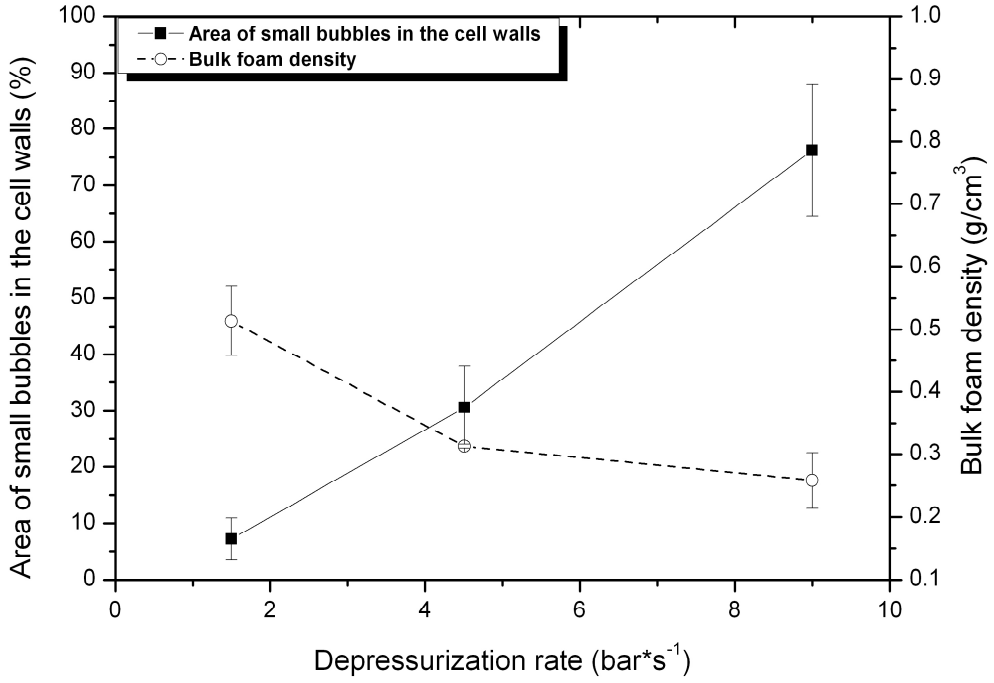

Figure 3.5. Average area fractions of small bubbles in the cell walls and bulk foam densities for three different depressurization rates using the PS/MMA 50:50 + 0.5 wt.-% DUDMA system.

3.3.4. Effect of initial monomer concentration

As mentioned in the previous section, it is possible that the small bubbles were nucleated in the cross-linked PMMA-rich domains in the cell wall. To confirm this speculation, the effect of the MMA concentration in solution on the cell structure was investigated. It was expected that a higher MMA concentration could increase the number or size of the PMMA rich-domain in the PS matrix and increase the number of small bubbles in the cell wall. Figure 3.6 shows SEM micrographs of foams prepared from three PS/MMA solutions with different ratios, 50:50, 33:67, and 15:85. The increase in the initial MMA concentration increases the number of micro-bubbles and

decreases the number density of large bubbles as shown in Fig. 6. Even though the number density of large bubbles decreased, their average diameter increased (Fig. 3.7), and the bulk foam density decreased from 0.26 $g \cdot cm^{-3}$ to 0.23 $g \cdot cm^{-3}$ by the increase in the percentage of the micro-bubble area (Figs. 3.8 and 3.9).

However, a further increase in the MMA concentration (PS/MMA 15:85) did not increase the number of micro-bubbles. Rather, the cell structure deteriorated due to the MMA monomer that was left in the PS even after polymerization (Fig. 3.6-e), and the elasticity of the polymer blends decreased due to the swelling effect of the residual monomer. Therefore, the system PS/MMA 15:85 was excluded from further investigations.

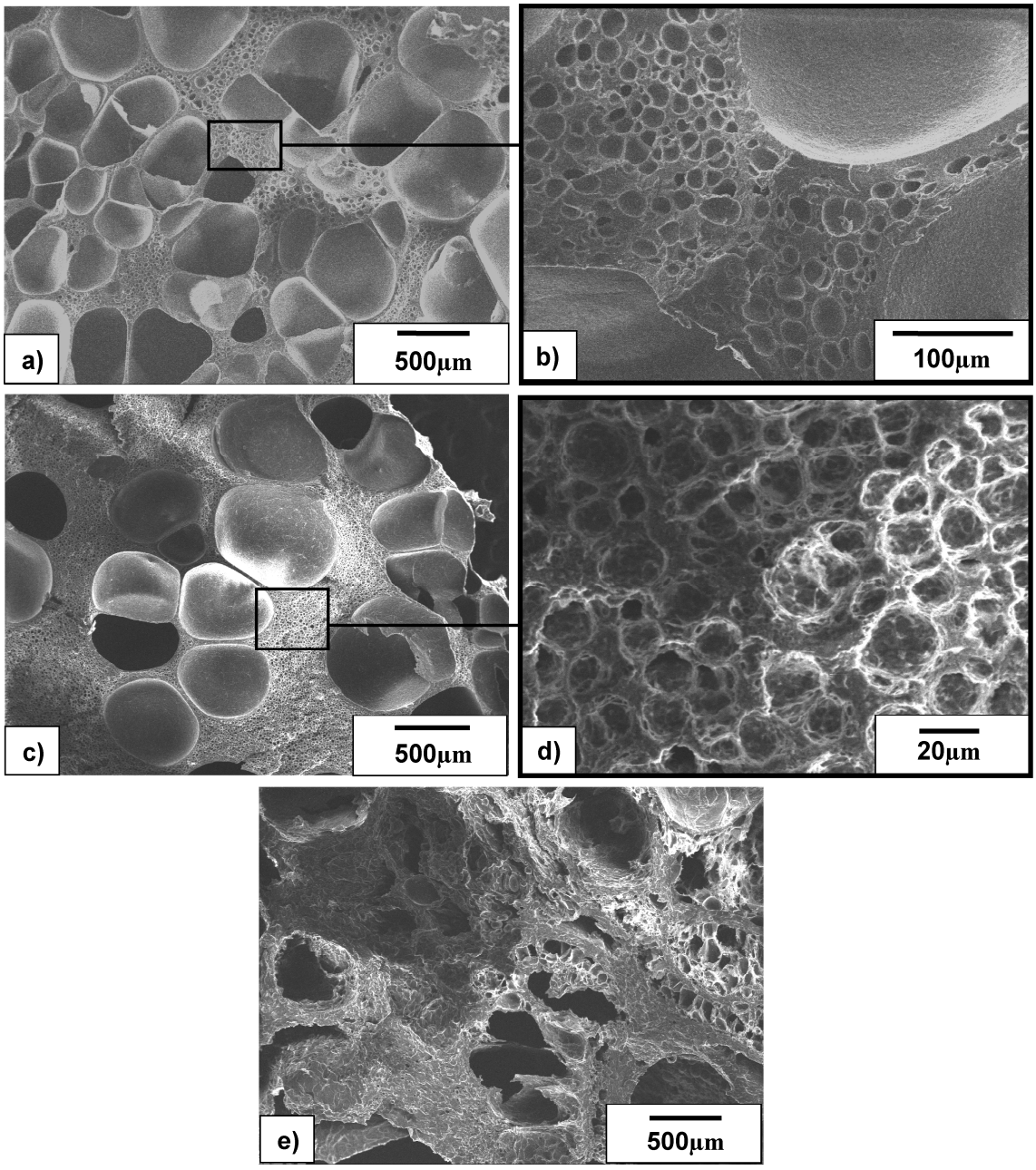

Figure 3.6. Different polymer-monomer systems foamed with the same depressurization rate dp/dt= 9 bar·s^{-1}. a) and b): PS/MMA 50:50 + 0.5 wt.-% DUDMA; c) and d): PS/MMA 33:67 + 0.5 wt.-% DUDMA; e) PS/MMA 15:85 + 0.5 wt.-% DUDMA.

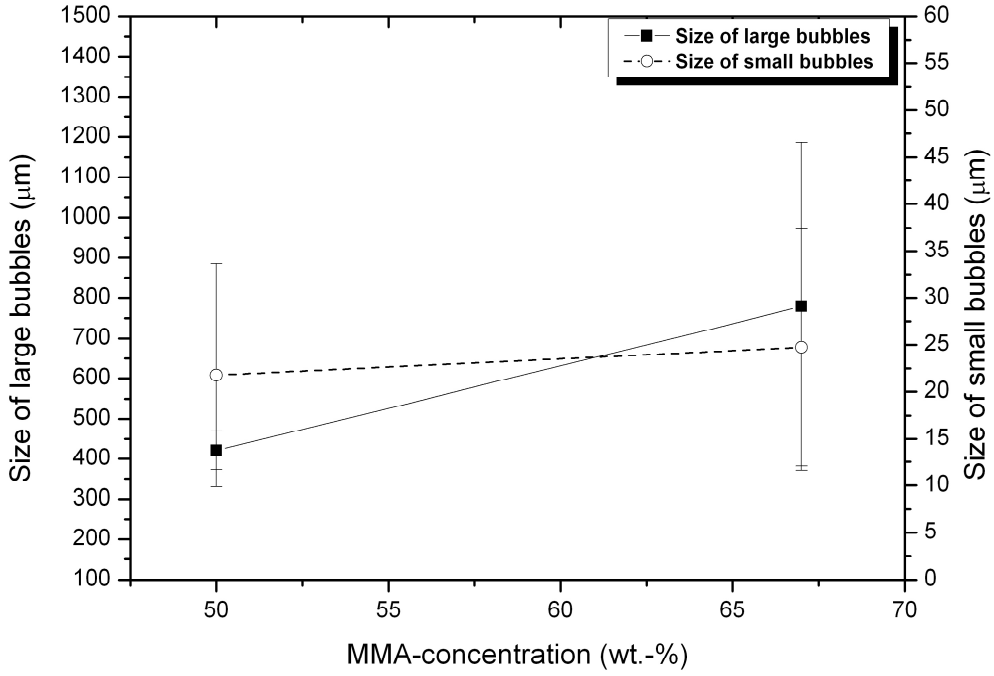

Figure 3.7. Average cell sizes of large and small bubbles for the following systems: PS/MMA 50:50 + 0.5 wt.-% DUDMA and PS/MMA 33:67 + 0.5 wt.-% DUDMA foamed with dp/dt= 9 bar·s^{-1}.

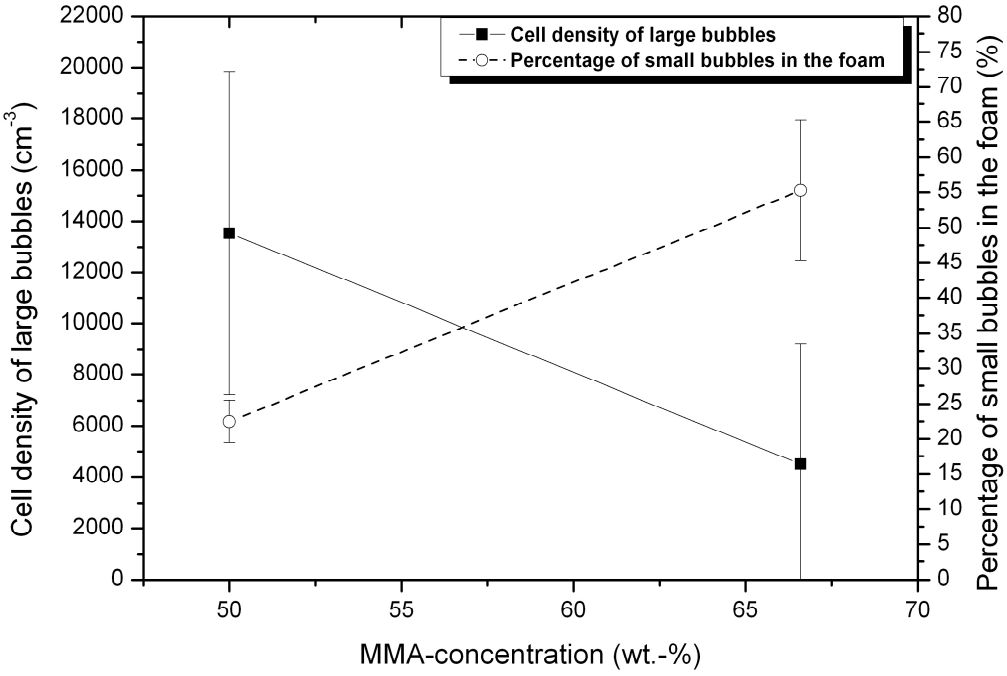

Figure 3.8. Average cell densities of the large bubbles for the following systems: PS/MMA 50:50 + 0.5 wt.-% DUDMA and PS/MMA 33:67 + 0.5 wt.-% DUDMA foamed with dp/dt= 9 bar·s^{-1}.

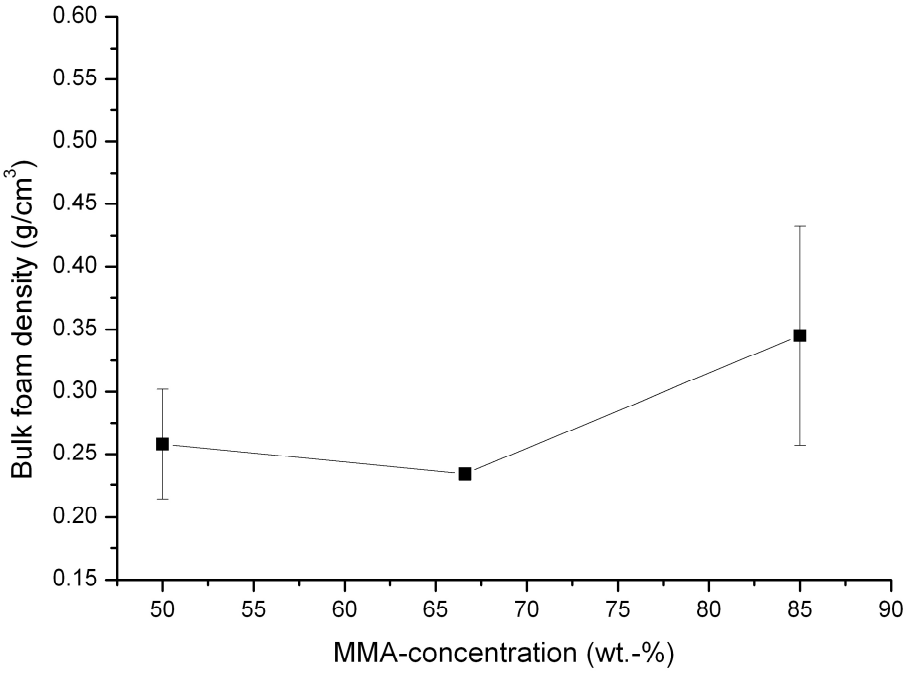

Figure 3.9. Average bulk foam densities for the following systems: PS/MMA 50:50 + 0.5 wt.-% DUDMA, PS/MMA 33:67 + 0.5 wt.-% DUDMA, and PS/MMA 15:85 + 0.5 wt.-% DUDMA foamed with dp/dt= 9 bar·s^{-1}.

3.3.5. Effect of cross-linking agent concentration

Figures 3.10 and 3.11 show the effect of the cross-linking agent concentration on the cell structure. The diameters of both the large and small bubbles decreased as the cross-linking agent concentration was increased. The average diameter of the large bubbles decreased from approximately 425 to 200 µm, and that of the small bubbles decreased slightly from 22 and 12 µm. Here, an increase in the DUDMA concentration suppressed the growth rate and nucleation of the small and large bubbles. As a result, the size of both types of bubbles decreased, and the percentage of the micro-bubble area also decreased. Consequently, the increase in the bulk foam density was further

enhanced from 0.25 g·cm^{-3} initially to 0.35 g·cm^{-3} as shown in Fig. 3.11.

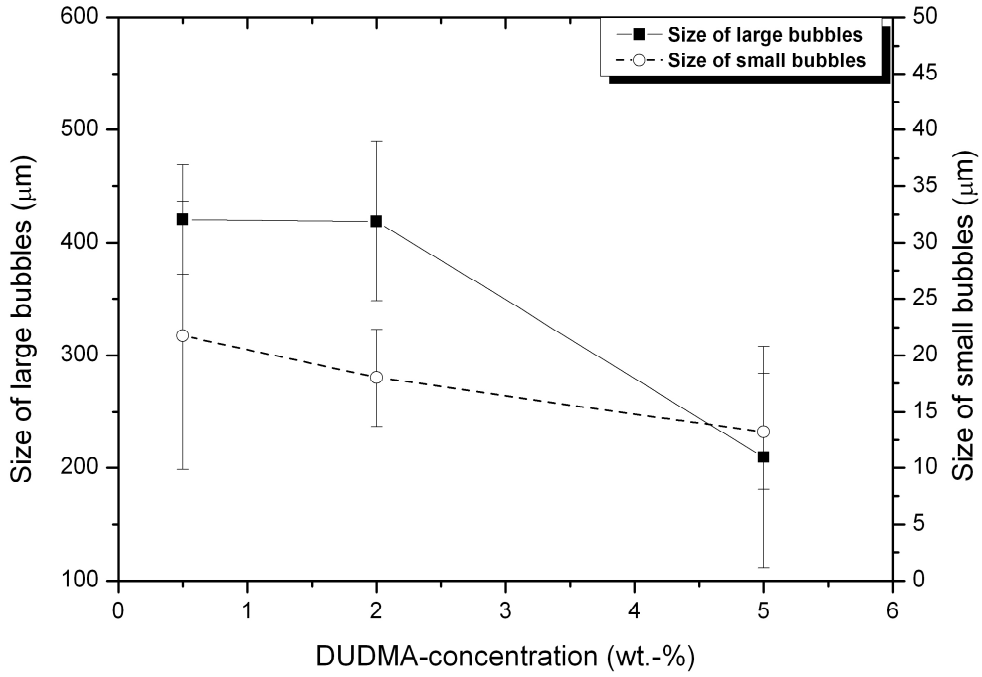

Figure 3.10. Average large and small bubbles of the following systems: PS/MMA 50:50 + 0.5 wt.-%, 2 wt.-%, and 5 wt.-% DUDMA. The applied depressurization rate was dp/dt= 9 bar·s^{-1}.

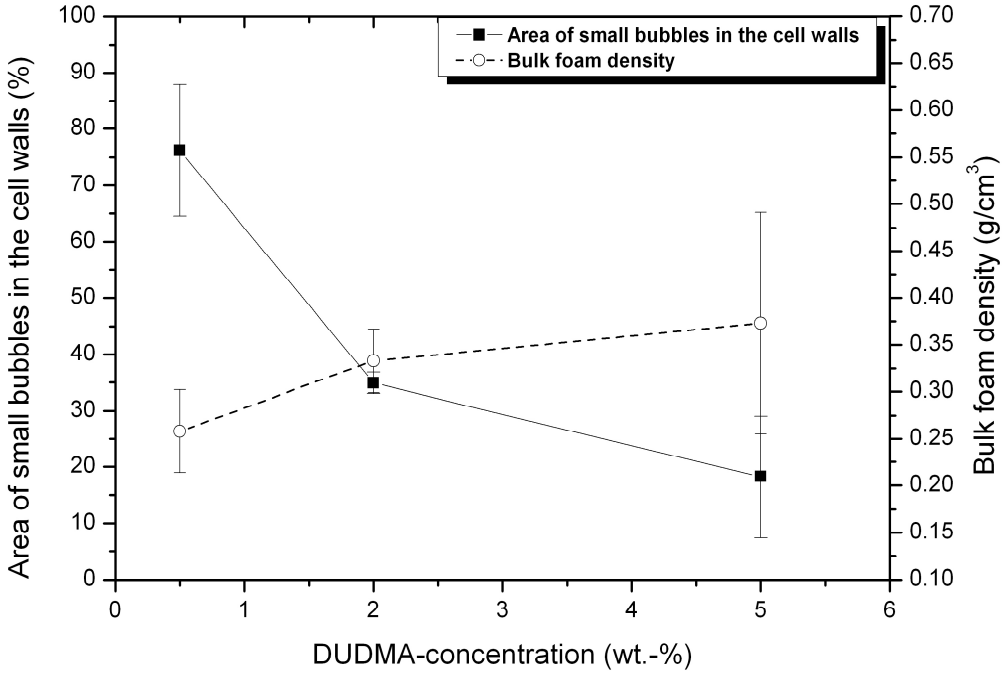

Figure 3.11. Average bulk foam densities and area of cell walls in which small bubbles were detected for the following systems: PS/MMA 50:50 + 0.5 wt.-%, 2 wt.-%, and 5 wt.-% DUDMA. The applied depressurization rate was $dp/dt = 9\ bar \cdot s^{-1}$.

3.4. Conclusion

Foams with a bimodal cell size distribution were prepared from PS/PMMA polymer blends, in which the small cells were 10-30 μm in diameter and were located in the wall of large cells 200-400 μm in diameter. By in-situ polymerization, highly dispersed, cross-linked, PMMA-rich domains were formed in the PS matrix and were used as sites of bubble nucleation. Because of the elasticity difference between the PMMA-rich domains and the PS matrix, secondary nucleation was induced in the PMMA-rich domains after the first bubble nucleation took place in the PS matrix. The elasticity of the PMMA-rich domains, as well as the bulk polymer sample, increased with the cross-linking agent concentration, and the size of both the large and small cells could be reduced by increasing the cross-linking agent concentration. The initial MMA monomer concentration in PS affected the cell morphology. With an increase in the MMA monomer concentration, the number of small bubbles that nucleated in the cell walls increased.

3.5. References

[1] L. Li, H. Yokoyama, T. Nemoto, K. Sugiyama, *Adv. Mater.* **2004**; *16*, 1226.

[2] T. Nemoto, J. Takagi, M. Ohshima, *Macromol. Mater. Eng.* **2008**; *293*, 574.

[3] T. Nemoto, J. Takagi, M. Ohshima, *Macromol. Mater. Eng.* **2008**; *293*, 991.

[4] J. S. Colton, N. P. Suh, *Polym. Eng. Sci*. **1987**; *27*, 485.

[5] N. S. Ramesh, D. H. Rasmussen, G. A. Campbell, *Polm. Eng. Sci.* **1994**; *34*, 1685.

[6] C. B. Park, D. F. Baldwin, N. P. Suh, *Polym. Eng. Sci.* **1995**; *35*, 432.

[7] B. Krause, H. J. P. Sijbesma, P. Munuklu, N. F. A. van der Vegt, M. Wessling, *Macromolecules* **2001**; *34*, 8792.

[8] Y. Fujimoto, S. S. Ray, M. Okamoto, A. Ogami, K. Yamada, K. Ueda, *Macromol. Rapid Commun.* **2003**; *24*, 457.

[9] P. C. Lee, G. Li, J. W. S. Lee, C. B. Park, *J. Cell. Plast.* **2007**; *43*, 431.

[10] P. C. Lee, H. E. Naguib, C. B. Park, J. Wang, *Polym. Eng. Sci.* **2005**; *45*, 1445.

[11] US. 6 174 471 (2001), The Dow Chemical Company MI, invs.: C.P. Park, B. Chaudhary, D. Imeokparia.

[12] P. C. Lee, J. Wang, C. B. Park, *Ind. Eng. Chem. Res.* **2006**; *45*, 175.

[13] C. B. Park, V. Padareva, P. C. Lee, H. E. Naguib, *J. Polym. Eng.* **2005**; *25*, 23.

[14] K. A. Arora, A. J. Lesser, T. J. McCarthy, *Macromolecules* **1998**; *31*, 4614.

[15] JP,11-552805, PCT/SP99/02177 (2001), Kaneka Co. ltd, invs.: T. Hayashi, O. Kobayashi, J. Fukuzawa, H. Fujiwara.

[16] L. E. Daigneault, R.Gendron, *J. Cell. Plast.* **2011**; *37*, 262.

[17] L. J. M. Jacobs, S. A. M. Hurkens, M. F. Kemmere, J. T. F. Keurentjes, *Macromol. Mater. Eng.* **2008**; *293*, 298.

[18] X.- L. Jiang, T. Liu, L. Zhao, Z.- M. Xu, W.- K. Yuan, *J. Cell. Plast.* **2009**; *45*, 225.

[19] Z.- M. Xu, X.- L. Jiang, T. Liu, G.- H. Hu, L. Zhao, Z.-N. Zhu, W.-K. Yuan, *J. Supercrit. Fluids* **2007**; *41*, 299.

[20] L. H. Sperling, *J. Polym. Sci., Macromol. Rev.* **1977;** *12*, 141.

[21] M. D. Elkovitch, D. L. Tomasko, J. L. Lee, *Polym. Eng. Sci.* **1999**; *39*, 2075.

[22] K. Okamoto, T. Ichikawa, T. Yokohara, M. Yamaguchi, *Eur. Polym. J.* **2009**; *45*, 2304.

[23] Y. Aoki, *Macromolecules* **1988**; *21*, 1277.

Chapter 4

Influence of Polyethylene Disperse Domain on Cell Morphology of Polystyrene Based Blend Foams

4.1. Introduction

Non-homogeneity and partly miscibility of polymer blends were exploited in chapters 2 and 3 to create open cellular foams and bimodal cellular structured foams, respectively. The idea behind them was to use blend morphology as a template of cell structure and control the onset timing of bubble nucleation and bubble collapse exploiting the differences in viscoelasticity of local domains from the matrix of the blend morphology. To obtain the fine sea-and-island morphology, IPN structure was prepared in both chapters 2 and 3. In this chapter, the idea of exploiting non-homogeneity of blend morphology and viscosity will be further investigated using the polymer blends obtained by simple melt mixing.

It is well known that the viscosity is a function of temperature. Therefore, by manipulating the foaming temperature, the viscosity of the disperse domain can be controlled. In this chapter, polystyrene (PS) - polyethylene (PE) blends were used where PE consisted a disperse domain. PE was chosen to make its melt viscosity lower than PS in molten state but make it higher than that of PS by setting the foaming temperature lower than T_m and higher than T_g of PS matrix.

Polystyrene was chosen as the base resin to foam because polystyrene foams are multifunctional materials in industry as well as in daily life. They are used, e.g., as

insulation panels for acoustic applications, base material for the preparation of food trays, as packaging material due to lower material costs than non-foamed plastics, for several applications in the field of heat insulation, and as damping material.

To prepare the foams, bubbles have to nucleate and grow in the polymer matrix. Two different mechanisms of bubble nucleation exist, i.e., homogeneous and heterogeneous nucleation. The nucleating performance of different substances has already been discussed extensively in many literatures [1-5]. For example, Hansen et al.[1] used finely- dispersed metal particles in a polymer melt to induce heterogeneous nucleation and decrease cell sizes. Ramesh and coworkers[2-3] conducted numerical calculation to study on the influence of polybutadiene rubber micro and nano particles for bubble nucleation. They have shown that the size of particle as well as the particle density per unit volume of matrix polymer has a significant impact on the nascent foam. Other researchers extended their investigations to the field of inorganic nano tubes and nano fibers. Shen et al.[4] could increase cell density by adding carbon nano fibers to a polystyrene matrix. They reported that good dispersion of the fibers in the matrix as well as the surface curvature of the particles could create foams with higher cell densities and lower cell diameters. Sharudin et al.[5] used polypropylene (PP) as a nucleating agent in polystyrene and polymethyl metahcrylate (PMMA) based blends. They conducted the foaming experiments at temperatures above glass transition temperature of PS and PMMA but below the melting temperature of PP. Cell size could be decreased and cell density increased as long as PP domains were well- dispersed and small in diameter enough to maintain a high surface to volume- ratio; moreover, they found out that heterogeneous nucleation was enhanced if surface tension between the matrix and the dispersed domains was increased.

In this chapter, polyethylene (PE) was used for heterogeneous nucleation site by setting foaming temperature at which the viscosity of PE domains could be higher than that of matrix. Then, the foaming temperature was set so that the viscosity of PE domains could be low enough for cell walls to break up and to make cell structure open.

4.2. Experimental

4.2.1. Materials

All of the blends in this study consisted of PS and PE, where the polystyrene was the matrix and a certain amount of polyethylene formed the dispersive domain. General purpose polystyrene (GPPS) provided by Dow Chemical with a weight averaged molecular weight Mw=208,000 g·mol^{-1} was chosen as our matrix polymer. Three different grades of polyethylene were used as the dispersive phase polymer. One was Dow DOWLEX™ 2047G, a linear low-density polyethylene (LLDPE) with a Melt Flow Index (MFI)= 2.3g·(10min)$^{-1}$. Another grade was Tosoh high-melt tension polyethylene (HMS-PE) that had a high melt strength, a MFI= 4.1g·(10min)$^{-1}$ and an average molecular weight Mw=73,000 g·mol^{-1}. The third PE was Tosoh Nipolon® Hard 4000, a high-density polyethylene (HDPE) with MFI= 5g·(10min)$^{-1}$ and a molecular weight of Mw=77,000 g·mol^{-1}.

4.2.2. Preparation of blends by melt mixing

All blends were prepared using a twin-screw extruder (ULTnano 05, TECHNOVEL, Japan). All temperatures at conveying, compression, metering, and die zones were set to 200 °C. The polymer pellets were mixed at a screw speed of 35 rpm for 15 minutes. Subsequently, the extrudate of the strands was ground in a freeze mill

(AS ONE, TPH-02, Japan) before compression molding by a mechanical hot press for additional 20 minutes at 200 °C. All samples were molded to be a plate approximately 1 mm in thickness. The blend ratios of the investigated samples are listed in Table 4.1.

Table 4.1. Weight ratios of polymer blends.

Dispersed / Matrix	LLDPE	HMS-PE	HDPE
GPPS	99/01	99/01	99/01
GPPS	95/05	95/05	95/05
GPPS	90/10	90/10	90/10

4.2.3. Rheological properties

The complex viscosities, $|\eta^*|$, of neat polystyrene and the blends were measured. Both torsion rectangular and 25 mm diameter parallel plate geometries were used to conduct dynamic temperature ramp tests with a rheometer (Advanced Rheometric Expansion System ARES). The temperature ramps were at a heating/ cooling rate of 2 °C·min^{-1} in two different temperature ranges. The torsion test was performed in the temperature range of 35 to 140 °C, while the parallel plate test was performed in the temperature range of 130 to 200 °C. The oscillation frequency was set to 1 rad·s^{-1} with 0.1% strain. The samples that were prepared for the torsion test were 11 mm in width, 1mm in thickness, and 32 mm in length. The samples for the parallel plate test were 25 mm in diameter and 1.5 mm in thickness. The gap of the parallel plates was set to 1 mm in the rheometer.

4.2.4. Thermodynamic characterization

DSC system (A Perkin Elmer Pyris 1) was used to analyze the thermal property, i.e., the glass transition temperature, T_g, and melting point, T_m, of GPPS and their blends with PE. The sample, ca. 10 mg in weight, was placed in a sealed aluminum pan. Then, a heating and cooling cycle between 40 °C and 240 °C was applied at the rates of 10 °C·min^{-1}.

4.2.5. Foaming of neat polystyrene and polymer blends

The pressure-quench batch foaming experiments were conducted using CO_2 as the blowing agent. Samples were placed in a 120 cm^3 autoclave and purged with 99.9% pure CO_2 (Showa Tansan Japan). The autoclave was then heated to the desired foaming temperature, either 90 °C, 115 °C, 130 °C, or 140 °C, while the pressure was increased to 10 MPa with CO_2. When the effect of the crystalline phase of PE on cell morphology was investigated, two different temperature profiles were applied to reach the desired foaming temperature: 1) the autoclave temperature was directly increased from room temperature to the desired temperature, or 2) the autoclave temperature was first increased to 215 °C to completely melt the crystals of PE and then cooled down to the desired foaming temperature.

The sorption time for CO_2 was set to 6 hours for all of the samples. Foams were prepared by rapidly releasing the autoclave pressure from 10 MPa to atmospheric over a period of 5 to 6 seconds.

4.2.6. Characterization of cell morphology - cell density and size

The cell morphology was observed using a scanning electron microscope (SEM, Tiny-SEM 1540 upgraded for higher magnification, Technex Co. Ltd., Japan). The obtained micrographs were analyzed by the image processing software, Image J. The cell density (N_f) was calculated by:

$$N_f = \left(\frac{n}{A}\right)^{1.5}. \quad (1)$$

Where n is the number of bubbles detected in the area A (cm^2) of each micrograph.

4.3. Results and Discussion

4.3.1. Rheological characterization

Two different types of rheological measurements were conducted for this section. First, values of the complex viscosity, $|\eta^*|$, of neat PS and all tested types of PE were measured in the temperature range from 35 to 140 °C. Figure 4.1 shows the measurement results. All three types of PE alone showed lower $|\eta^*|$ than PS at temperatures lower than 100 °C, which is the glass transition temperature of PS. The absolute value of the complex viscosity of PS remained nearly constant at approximately $2x10^9$ Pa·s until the temperature exceeded its glass transition temperature, 100^oC. $|\eta^*|$ of HMS-PE, HDPE, and LLDPE decreased constantly with the increase of temperature. When crystals began melting at a temperature around 120 °C, the absolute values of the complex viscosity of PEs dropped drastically. LLDPE shows the lowest viscosity among PEs in the entire temperature range, and HMS-PE shows the second

lowest viscosity.

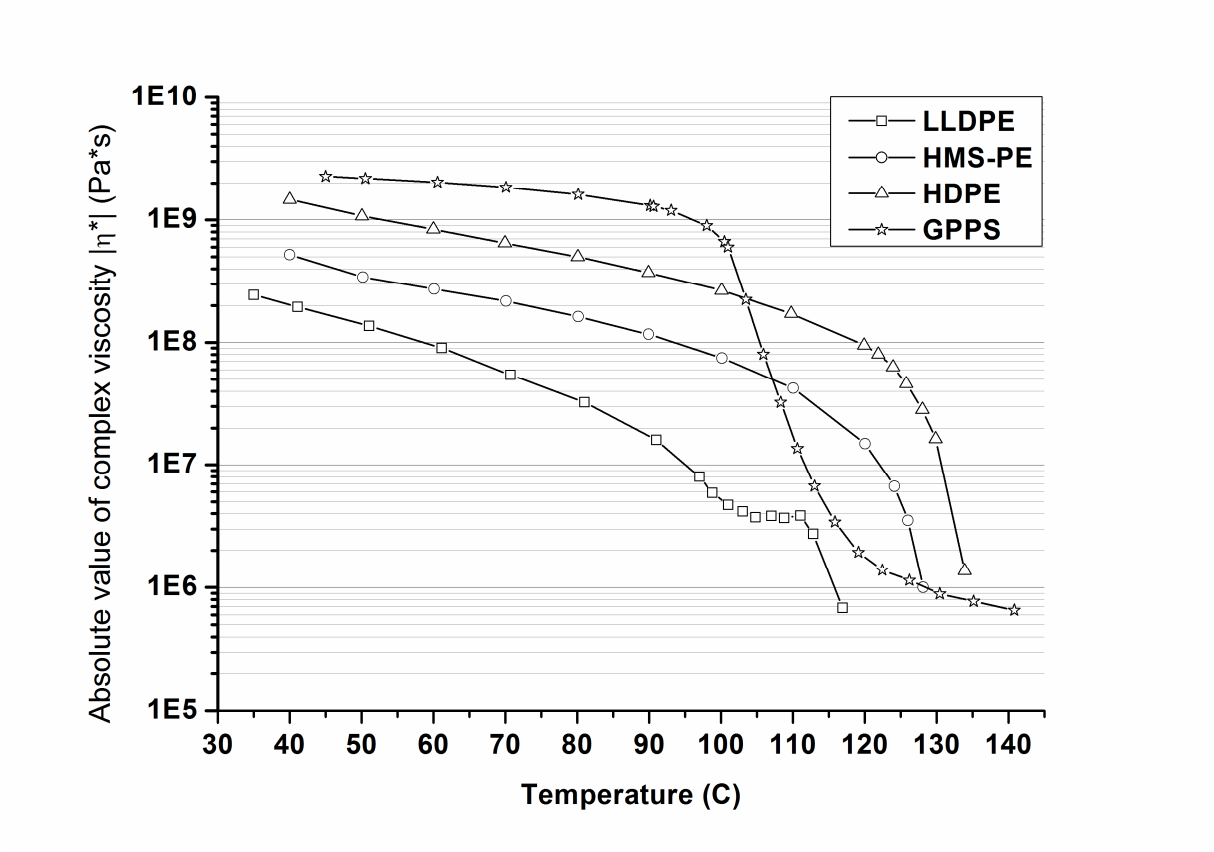

Figure 4.1. The absolute values of complex viscosities of neat GPPS, HMS-PE, HDPE, and LLDPE at temperatures in the range of 35 and 140 °C.

4.3.2. Influence of remaining PE crystals on cell morphology

To confirm that PE crystals were completely molten over 130 °C, DSC analysis, rheological measurements and optical investigations were conducted for GPPS/HMS-PE, GPPS/HDPE, and GPPS/LLDPE blends. Figure 4.2 shows the results of the DSC measurements of these blends with 90/10 PS/PE blend ratio. All blend samples showed an inflection point of approximately 105 °C, which corresponds to the T_g of PS, and a melting peak of approximately 125 °C, which is associated with polyethylene crystals.

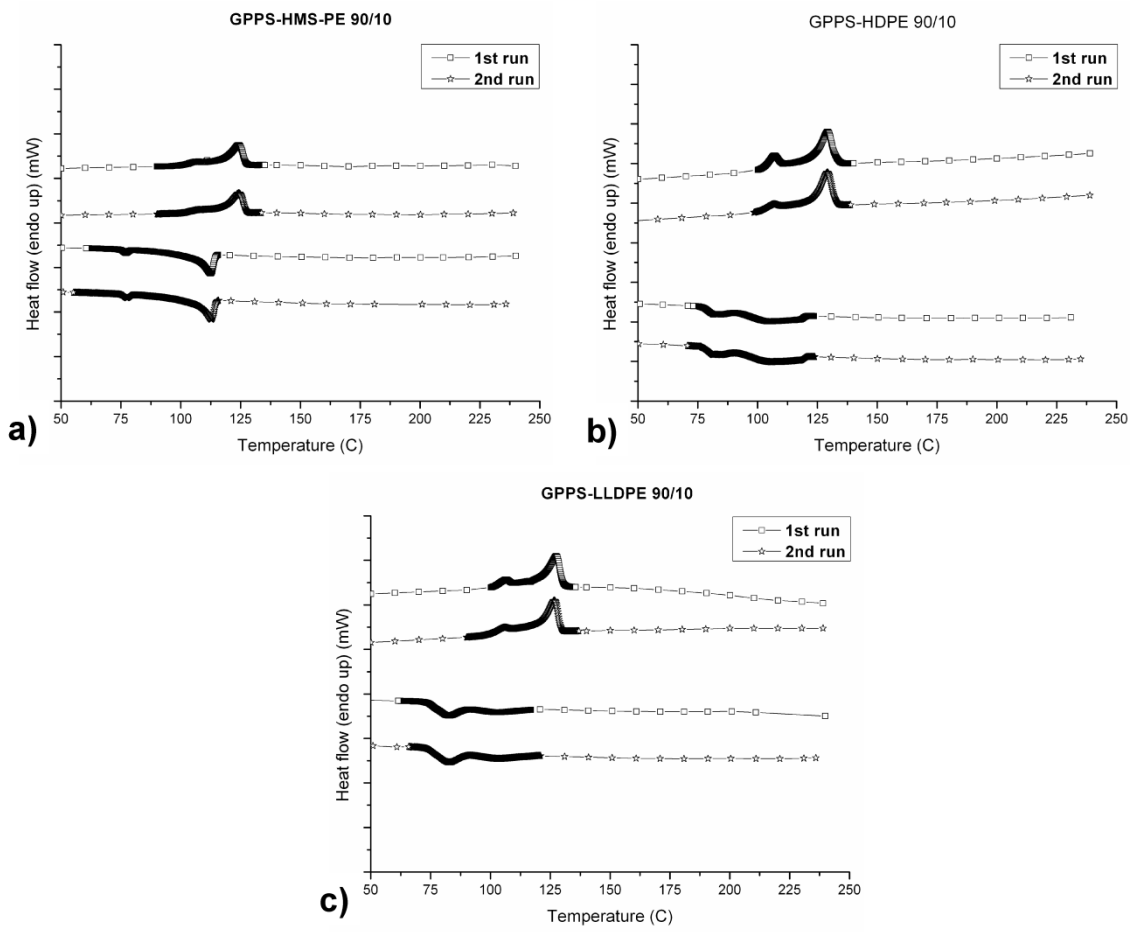

Figure 4.2. DSC heat curves of a) GPPS/HMS-PE, b) GPPS/HDPE, and c) GPPS/LLDPE.

Figure 4.3 shows the complex viscosity-temperature curves of three different blends. The complex viscosity was measured with a heating/cooling cycle between 130 and 200 ^{o}C at a rate of 2 ^{o}C/min. As seen in Figures 4.3-b and 4.3-c, the hysteresis was not significant, and the differences were negligible especially for the blends of b) GPPS/HDPE and c) GPPS/LLDPE. Both the DSC and the rheology data indicated that PE crystals in blend were molten or remained too small to affect the rheological properties once the blends were heated to over 130 ^{o}C.

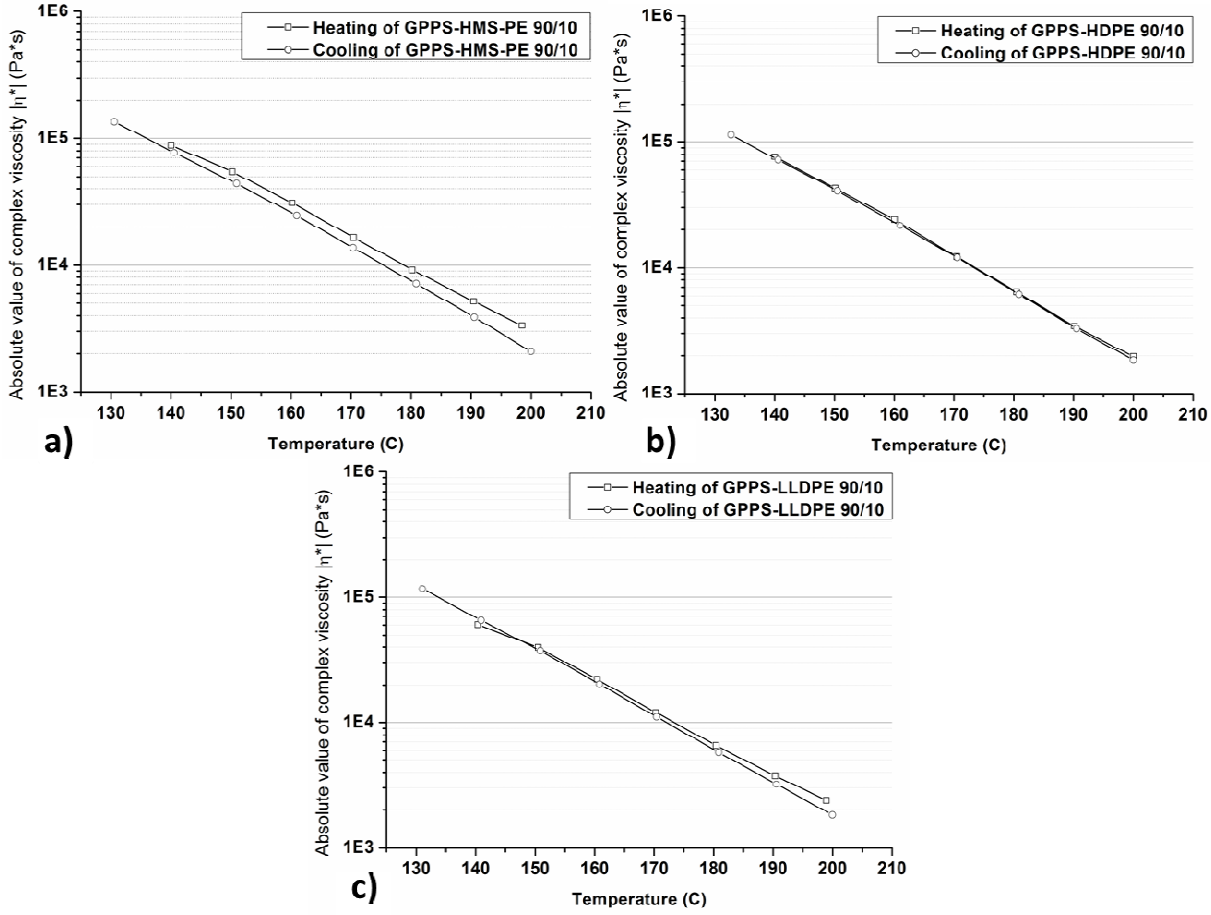

Figure 4.3. Absolute value of complex viscosities of a) GPPS/HMS-PE (90/10), b) GPPS/HDPE (90/10), and c) GPPS/LLDPE (90/10) measured in a heating and cooling cycle.

Two different temperature profiles were employed for foaming to observe the effect of crystallinity on the cell morphology of foamed blends at temperatures higher than 130 ^{o}C. In the first temperature profile, the samples were placed in the autoclave and purged with CO_2 at room temperature. Then, the temperature of the autoclave was increased from room temperature to 130 ^{o}C while pressurizing with CO_2 to 10 MPa. The temperature and the pressure were kept constant for 6 hours to saturate the sample with CO_2. Then, the samples were foamed at 130 °C and immediately cooled down. In the

second temperature profile, while controlling the pressure to 10 MPa, the temperature of the autoclave was increased from room temperature to 215 ^{o}C, which took approximately 30 minutes, and cooled down to 130 °C within approximately one hour. The samples were kept in contact with 10 MPa CO_2 for the remaining 4.5 hours before the autoclave was depressurized. If the crystals remain and affect the foaming behavior at temperature over 130 ^{o}C, cell sizes and cell density should be significantly different. Figure 4.4 shows the SEM micrograph of the cross sectional area of the blend foamed at 130 ^{o}C after being thermally treated with two different temperature profiles. Figures 4.4-a, -c, and -e show (a) GPPS/HMS-PE (90/10), (c) GPPS/HDPE (90/10), and (e) GPPS/LLDPE (90/10) blends foamed at 130°C with the first temperature profile. Figures 4.4-b, -d, and -f show (b) GPPS/HMS-PE (90/10), (d) GPPS/HDPE (90/10), and (f) GPPS/LLDPE (90/10) foamed at 130 ^{o}C after being treated with the second temperature profile. It can be observed that the difference in cell size is subtle. There is some difference observed in the cell size of the foamed GPPS/LLDPE: the cell sizes of the blend foamed using the first temperature profile (Figure 4.4-e) were smaller than those foamed using the second temperature profile (Figure 4.4-f). This difference might indicate the effect of the remaining PE crystals in the blend, but any effect was very small.

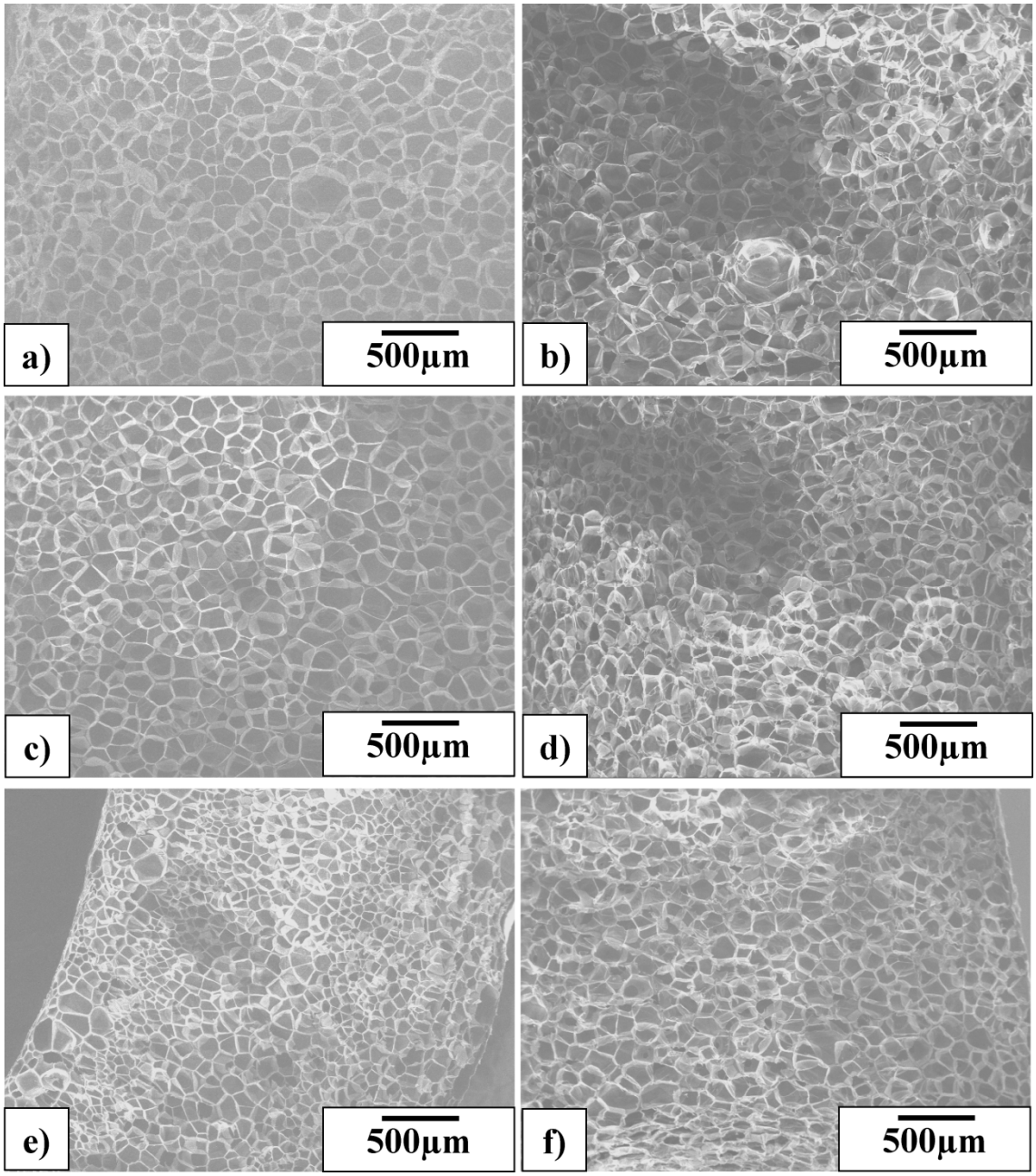

Figure 4.4. Comparison between the samples foamed at 130°C and the samples which were firstly heated up to 215°C in order to make sure that all crystals of polyethylene were in the molten state. Figures 4.4-a to 4.4-c refer to HMS-PE (Fig. 4.4-a), HDPE (Fig. 4.4-c), and LLDPE (Fig. 4.4-e). A similar cell structure could be obtained after melting HMS-PE (Fig. 4.4-b), HDPE (Fig. 4.4-d), and LLDPE (Fig. 4.4-f).

4.3.3. Influence of polyethylene viscosity on cell morphology

To clarify the influence of the PE disperse domain on the cell morphology of blends at lower temperature ranges (lower than the T_m of PE), the blends were foamed at two different temperatures: 90 and 115 ^oC. These foaming temperatures were chosen because of the viscosity differences between the disperse domain and the matrix. As shown in Figure 4.1, the neat PS has a higher complex viscosity than those of the three PEs at temperatures lower than 105 °C. A sudden reduction in complex viscosity was detected in PS when the temperature exceeded 110 °C. In the temperature range from 105 to 125 ^oC, the absolute values of the complex viscosities of HDPE and HMS-PE were higher than that of GPPS. Accordingly, the foaming temperature, 90 ^oC, was chosen as a temperature wherein the complex viscosity of the matrix (PS) was higher than those of disperse domain (PE). The other temperature, 115^oC, was chosen as a temperature wherein the complex viscosity of the matrix was lower than the complex viscosities of the PEs. These foaming temperatures were realized by simply increasing the autoclave temperature from room temperature to the specified temperatures while the autoclave was being pressurized with CO_2.

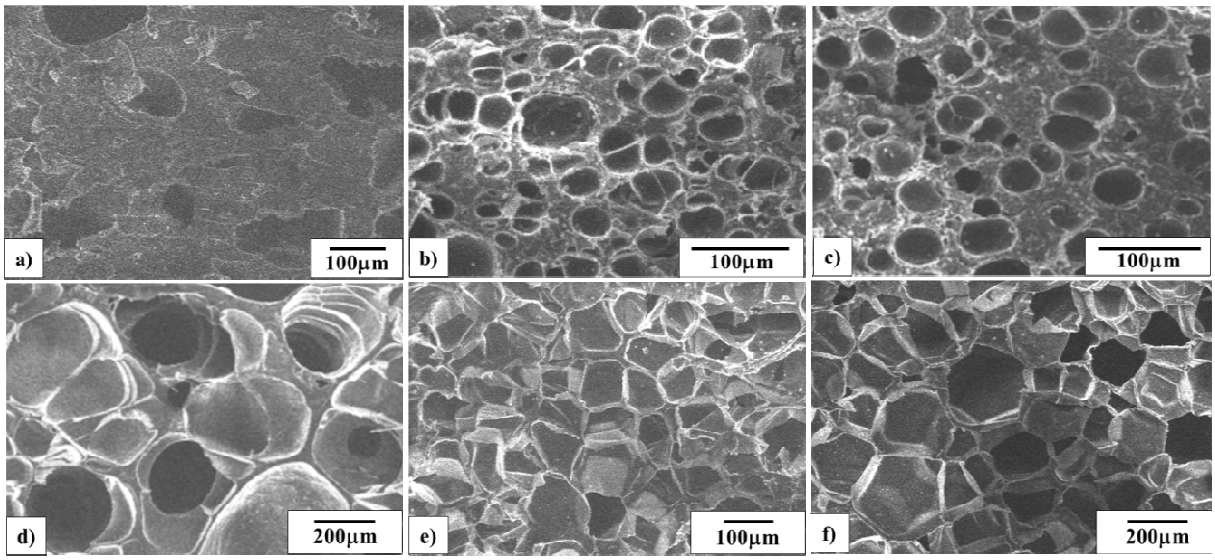

Figure 4.5. SEM micrographs of the blend foamed at 90 °C (4.5-a to 4.5-c) and 115 °C (4.5-d to 4.5-e). (4.5-a, 4.5-d): neat GPPS, (4.5-b, 4.5-e): GPPS/HDPE (90/10), (4.5-c, 4.5-f): GPPS/HMS-PE (90/10).

Table 4.2. Averaged cell diameters of the neat GPPS and blend foams.

Foaming Temperature (°C)	Neat GPPS; averaged cell diameter (μm)	GPPS/HDPE 90/10; averaged cell diameter (μm)	GPPS/HMS-PE 90/10; averaged cell diameter (μm)
90 °C	175	29.75	41.46
115 °C	384.18	94.12	156.34

Figure 4.5 shows SEM micrographs of the cross-sectional area of the neat GPPS, GPPS/ HDPE (90/10), and GPPS/HMS-PE (90/10) foamed at 90 and 115 °C. At the lower foaming temperature, microcellular foams were prepared from the GPPS/HDPE and GPPS/HMS-PE blends, while the foam of neat GPPS could not be foamed uniformly as shown in Fig. 4.5-a. The average cell size was measured from

SEM micrographs, and the results are listed in Table 4.2. The cell size increased at each polymer as the foaming temperature increased. The cell size of GPPS/HDPE foam was smaller than that of GPPS/HMS-PE foam. This phenomenon could be caused by the viscosity difference between HDPE and HMS-PM. As shown in Figure 4.1, the absolute value of the complex viscosity of HDPE was higher than that of HMS-PE. The higher complex viscosity might make the bubble growth slower and the cell size smaller. However, the higher elongational viscosity of HMS-PS could not be exploited in the low expansion foams to make the cell size smaller and the cell wall thinner.

Comparing the cell morphology of the neat GPPS with those of the blend foams, it was found that the PE disperse domain could enhance bubble nucleation at both temperatures. The similar results were obtained at the blend with different blend ratios. However, it was not certain whether the viscosity difference between the matrix and disperse domain polymers is needed for enhancement of bubble nucleation. As Sharudin et al.[5] indicated, the higher interfacial tension between the matrix and disperse phase polymers might be a major parameter for controlling bubble nucleation in blend foams.

To more clearly see the effect of the viscosity difference between the matrix and disperse domain, GPPS/LLDPE blends were foamed at three different temperatures: 90 °C, 115 °C, and 130 °C. At both of the lower temperatures, the absolute value of complex viscosity of LLDPE was lower than that of PS. In particular, at 115 °C, HMS-PE and HDPE showed a higher complex viscosity than the matrix polymer GPPS, while LLDPE showed a lower complex viscosity. The batch-pressure quench foaming experiments of GPPS/LLDPE blends with three different blend ratios were conducted at three different temperatures: 90, 115, and 130 °C. The average cell sizes and cell

densities of the obtained foams were measured and are shown in Figures 4.7- 4.9. For comparison, cell sizes and densities of GPPS foamed at 90, 115, and 130 °C were also measured and are shown in Figure 4.6.

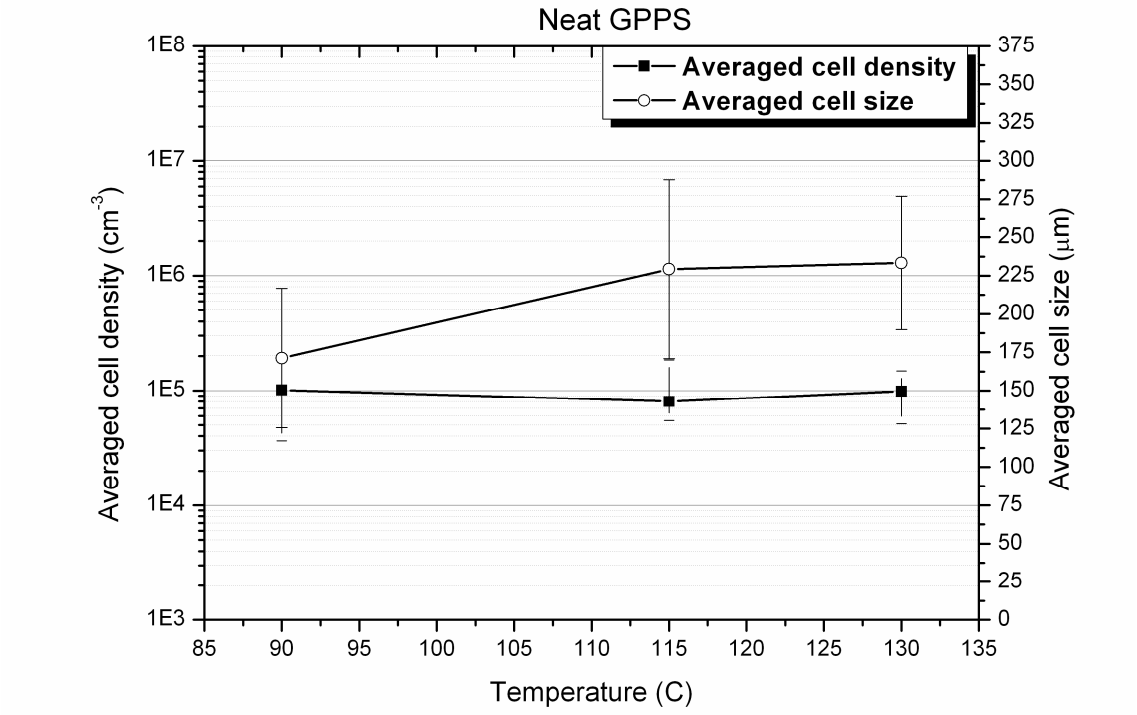

Figure 4.6. Averaged cell density and cell size of neat GPPS foams prepared at 90 °C, 115 °C, and 130 °C.

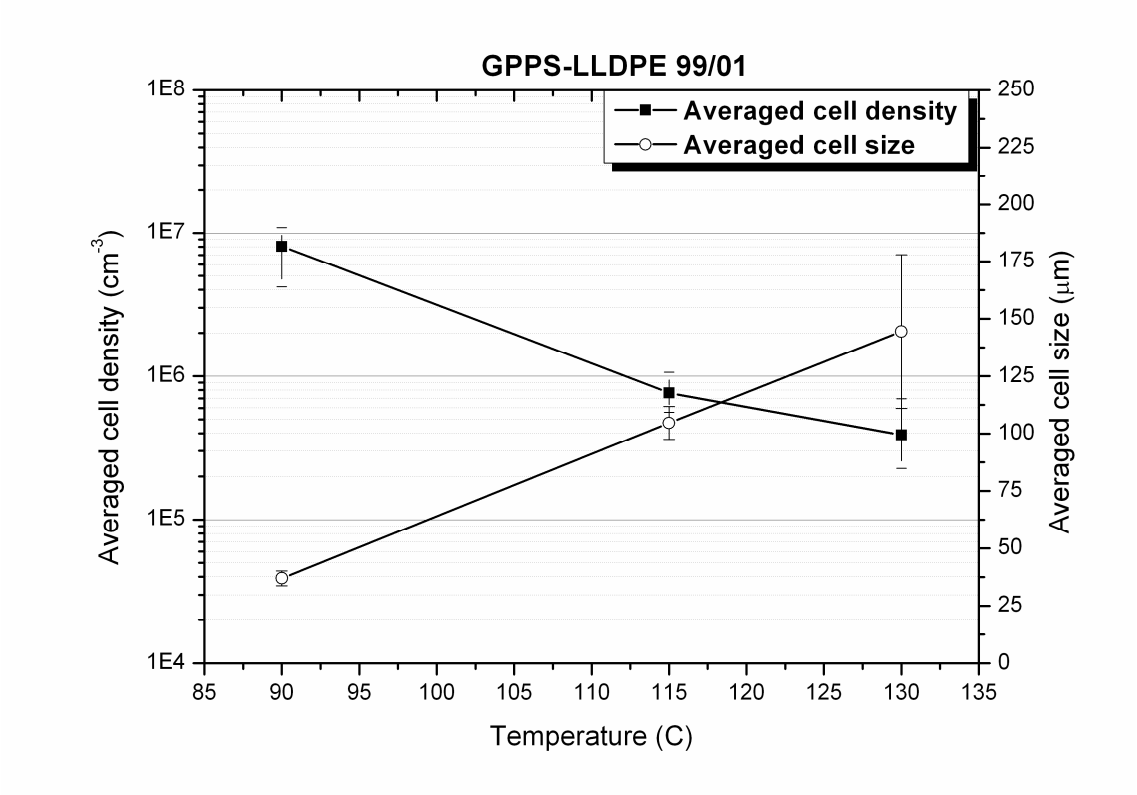

Figure 4.7. Averaged cell density and cell size of GPPS/LLDPE (99/01) foams prepared at 90 °C, 115 °C, and 130 °C.

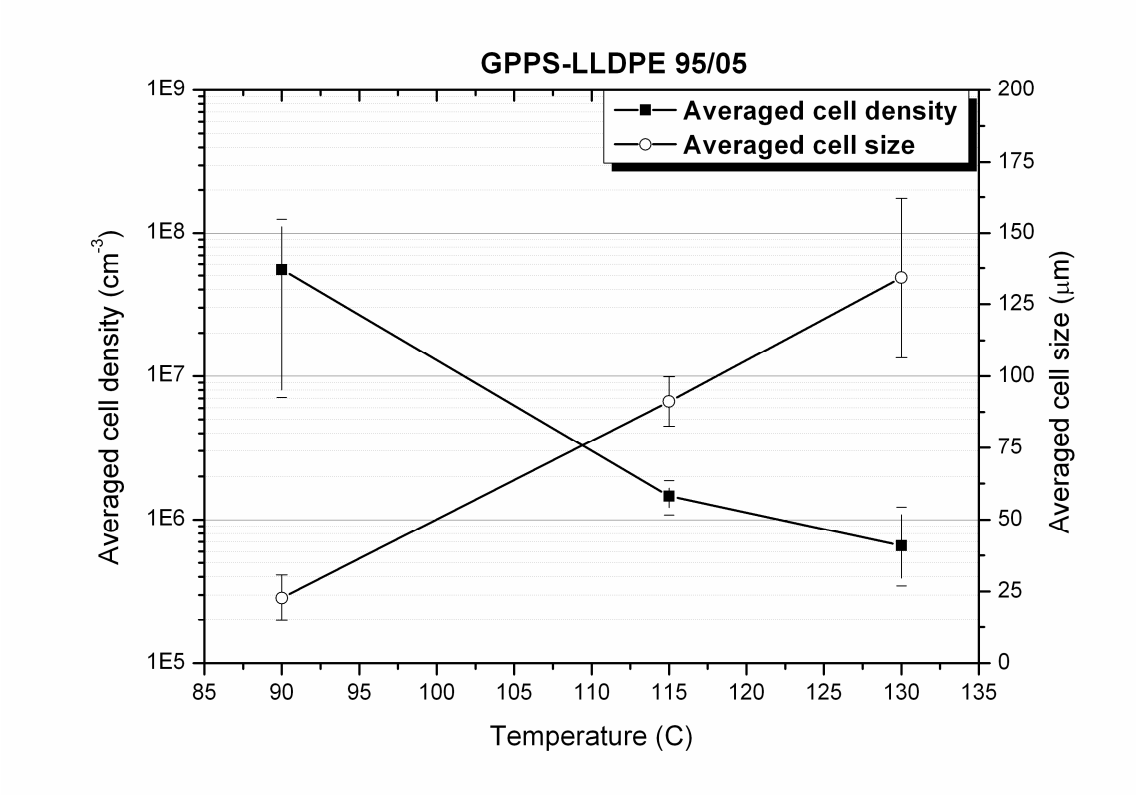

Figure 4.8. Averaged cell density and cell size of GPPS/LLDPE (95/05) foams prepared at 90 °C, 115 °C, and 130 °C.

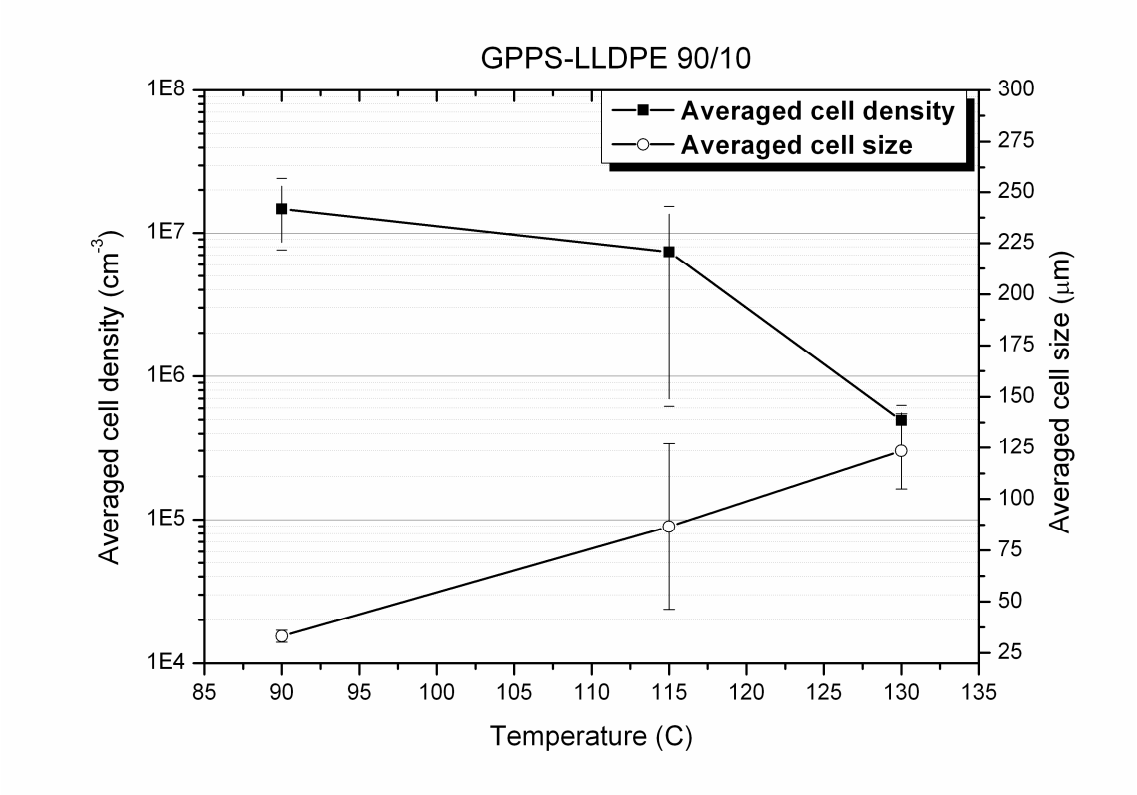

Figure 4.9. Averaged cell density and cell size of GPPS/LLDPE (90/10) foams prepared at 90 °C, 115 °C, and 130 °C.

For GPPS/LLDPE blends and for GPPS alone, as the foaming temperature increased, the complex viscosity decreased and the bubble growth was less suppressed. Consequently, the cell size was increased as shown in Figures 4.6- 4.9. The cell densities of the GPPS/LLDPE blend decreased as the foaming temperature increased. Comparison of the neat GPPS foam with the GPPS/LLDPE blend foams clearly shows that the GPPS/LLDPE blend foams had a much higher cell density than the GPPS foams at any temperature and any blend ratio. It is apparent that the disperse PE domain plays a role as a bubble nucleating agent in blends, and it could thus increase the cell density and decrease the cell size. The results were very similar to the foaming behaviors of GPPS/HMS-PE and GPPS/HDPE blends. Even at the foaming temperature

115 ^{o}C, we could not find any prominent features of cell morphology caused by the viscosity difference between the matrix and disperse polymers. It could be concluded that the enhancement of bubble nucleation might not be associated with the differences in viscosity between matrix and disperse domain polymers but rather, it might be primarily determined by interfacial tensions between matrix and disperse domain polymers.

The result was different when the foaming temperature was increased to 130 ^{o}C and higher. Over 130 ^{o}C, the absolute values of complex viscosities of all blends were lower than 10^5 Pa·s, which made it difficult for microcellular foam to be formed. Figures 4.10 and 4.11 show the cell sizes and densities of the three different PS/PE blends with the same blend ratio, 90/10, foamed at 130 and 140 °C. Interestingly, the averaged cell size was reduced and the cell density was increased by increasing the foaming temperature from 130 to 140 °C. The reduction of cell size and the increase of cell density were due to formation of small pores on the wall of large cells. Figure 4.12 shows SEM micrographs of the three different PS/PE blends foamed at 140 °C and shows the existence of interconnecting pores on the cell wall. Table 4.3 shows the average wall thickness of blends foamed at both 130 and 140 °C. The open cellular structure was observed in all three blend foams. Wong et al.[6] reported similar results for PS/LLDPE blend foams: A significant increase in bulk foam density was measured for the samples foamed at 127 °C, where a significant increase in the number of open cell was observed. In our study, the degree of cell opening varied with the grade of PE. The degree of cell opening was associated with the molecular architecture of PE, i.e., melt tension (elongational viscosity). LLDPE, which has the lowest complex viscosity among the investigated PE, showed the thinnest cell wall and the highest degree of cell wall

opening. For HMS-PE, which has a higher degree of elongational viscosity, the cell wall thickness was not changed by the temperature increase and the degree of cell opening was not increased with the increase of the foaming temperature. The dispersed PE domains are surrounded by PS matrix, and they are the weakest points that tend to be broken up during bubble expansion. As the viscosity of PE was lower, the degree of cell opening increased. However, the higher elongational viscosity could prevent the cell wall from opening.

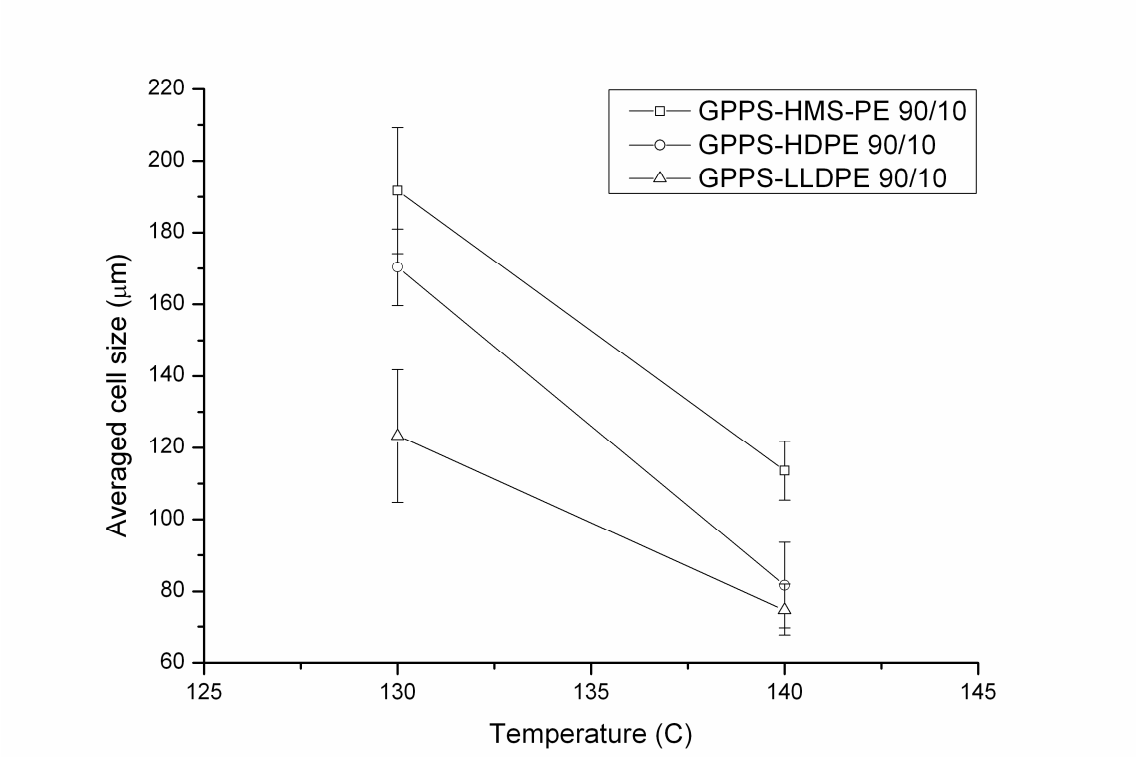

Figure 4.10. Averaged cell sizes of all blend systems containing 10 wt.-% PE foamed at 130 °C and 140 °C, respectively.

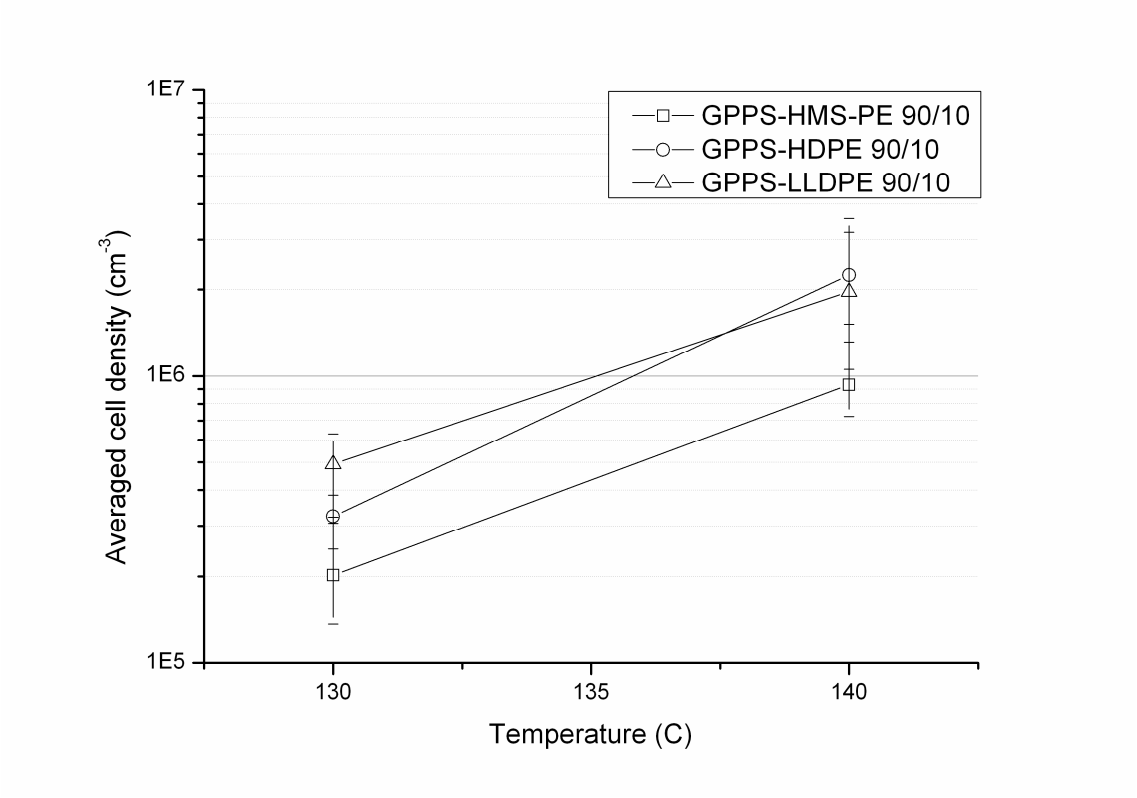

Figure 4.11. Averaged cell densities of all blend systems containing 10 wt.-% PE foamed at 130 °C and 140 °C, respectively.

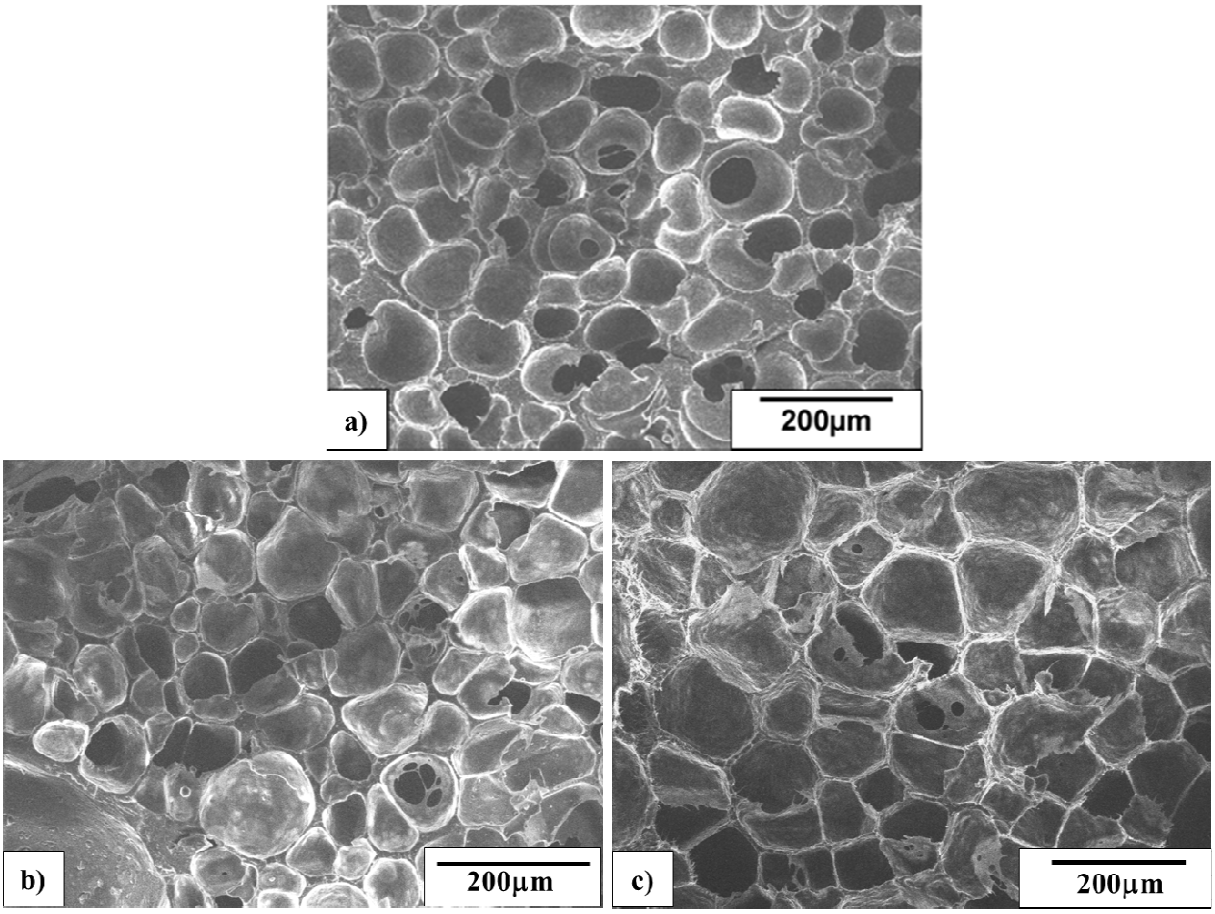

Figure 4.12. SEM- Micrographs of a) GPPS/LLDPE, b) GPPS/HDPE, and c) GPPS/HMS-PE 90/10 blend ratio, foamed at 140 °C.

Table 4.3. Averaged cell wall thickness of all blends with 10 wt.-% PE content foamed at 130 °C and 140 °C, respectively.

Temperature (°C)	GPPS-HDPE	GPPS-HMS-PE	GPPS-LLDPE
130	18.34	15.26	16.41
140	12.53	15.46	11.4

4.3.4. Influence of polyethylene concentration

To investigate the effect of PE concentration in blends on cell morphology foamed at higher temperatures, the blend samples with different polyethylene concentrations were foamed at 130 °C. Figures 4.13 – 4.15 show the average cell sizes and densities for the foamed blends.

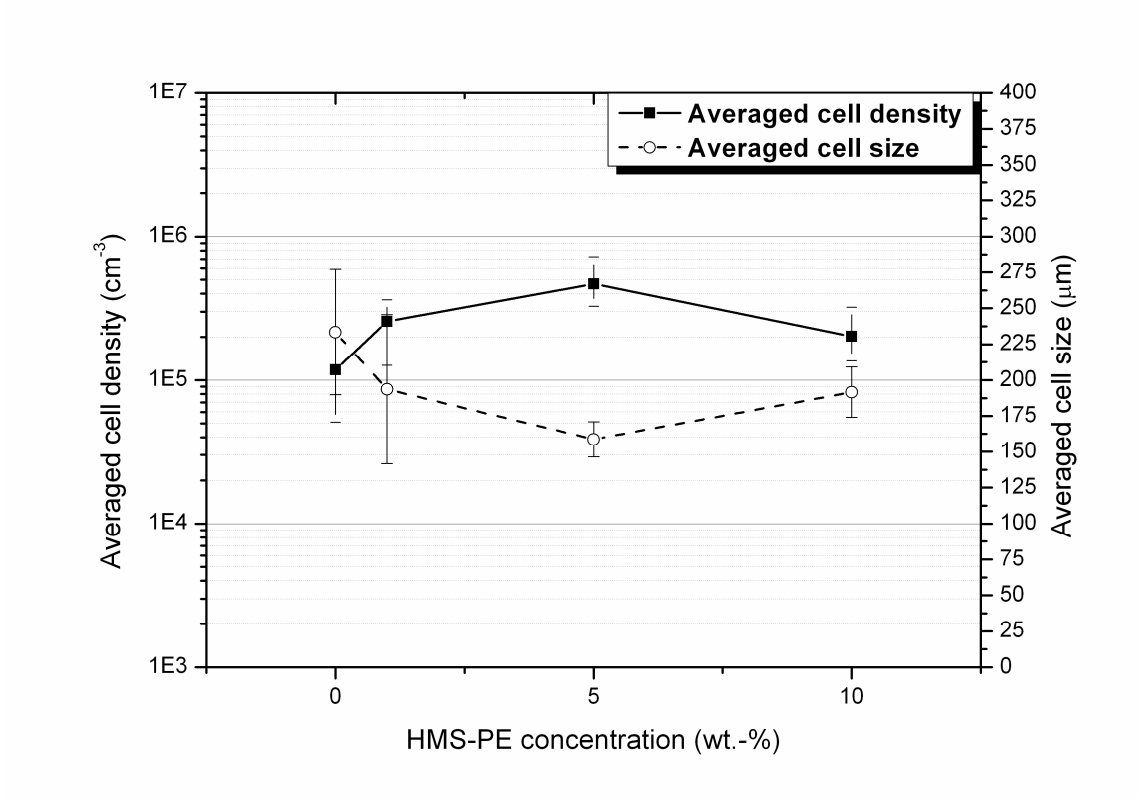

Figure 4.13. Averaged cell density and cell size of GPPS/HMS-PE 90/10 blends with different blend ratios (foamed at 130 °C).

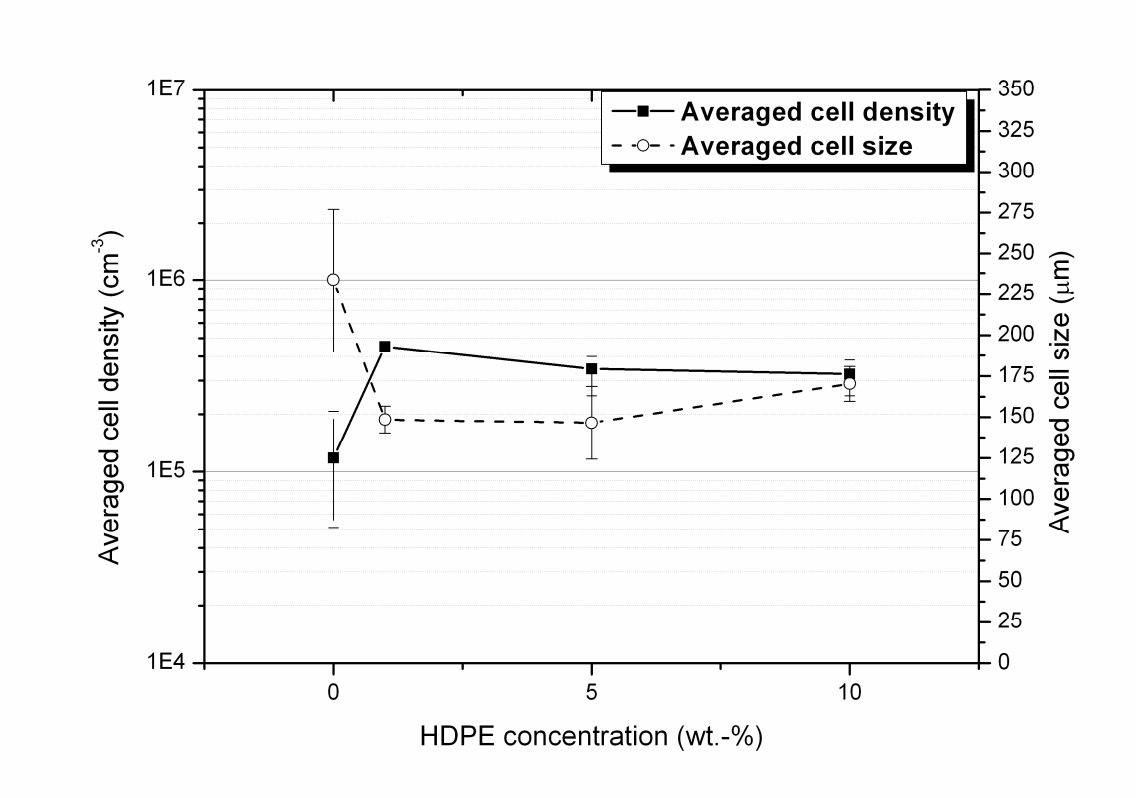

Figure 4.14. Averaged cell density and cell size of GPPS/HDPE 90/10 blends with different blend ratios (foamed at 130 °C).

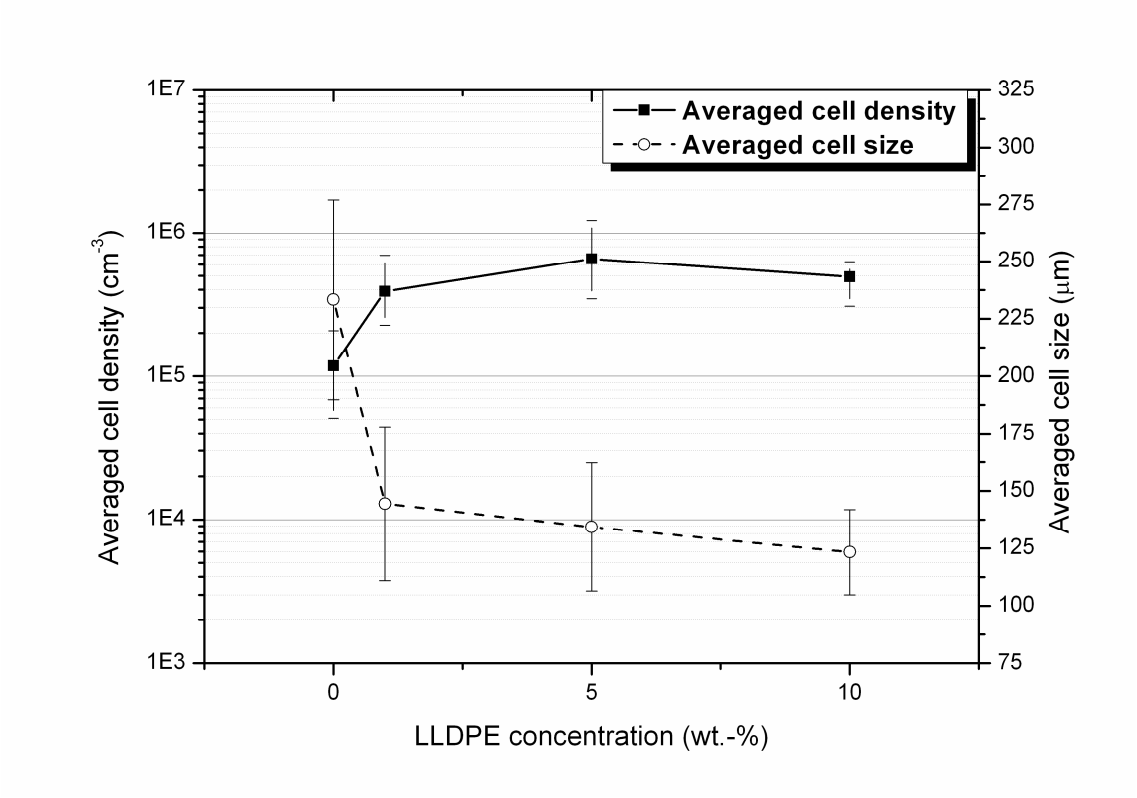

Figure 4.15. Averaged cell density and cell size of GPPS/LLDPE (90/10) blends with different blend ratios (foamed at 130 °C).

The average cell density of the neat GPPS foam was approximately 10^5 cm^{-3} with an average cell diameter of 240 μm. The blend of PE in PS increased the cell density for all concentrations. The maximum cell density was approximately $4x10^5$ cm^{-3} for 5% HMS-PE (Fig. 4.13) and 1% HDPE (Fig. 4.14). For the PS/LLDPE, the cell density could be increased to $6x10^5$ cm^{-3} with 5 weight %, as shown in Figure 15. As seen in Figures 13-15, the cell density did not increase monotonically with increasing PE content. The similar effect of PE content was observed in blends foamed at temperatures lower than 115 ^oC (Figures 7-9).

4.4. Conclusion

The formability of PS and PE blends was examined by discussing the effect of the PE domain on cell morphology. Three different grades of polyethylene, High Melt Strength PE (HMS-PE), High Density PE (HDPE), and Linear Low Density PE (LLDPE), were used with different PS/PE blend ratios in foaming experiments. We investigated how strongly the interfacial tensions and viscosity differences between PE and PS affected the cell size and cell density. The foaming temperature was changed in the range of 90 to 140 °C to control the degree of viscosity difference between the matrix and disperse domain polymers as well as the absolute value of the PE complex viscosity. At all foaming temperatures in the investigated temperature range, the blend of PE could enhance bubble nucleation and increase the cell density. The viscosity differences between the matrix and disperse domain polymers did not play a major role in enhancing bubble nucleation in the temperature range of 90 to 130 ^{o}C, where the absolute values of the complex viscosity of both matrix and disperse domain polymers were higher than 10^6 Pa·s. However, the viscosity of the disperse domain plays an important role in cell opening at the higher foaming temperatures where the absolute values of the complex viscosity of PS, PE and their blends were lower than 10^5 Pa·s. When the foam expansion ratio was increased with the increase in cell density, the cell walls became thinner and the disperse domain with lower viscosity opened the cell walls. A higher melt-tension, i.e., a high elongational viscosity of HMS-PE, could prevent the cell wall from opening. These experimental results show that it would be difficult to make an open microcellular foam by simply blending a polymer with lower or higher viscosity than the matrix polymer, especially the polymers with shear viscosities higher than 10^6 Pa·s. In our study, the viscosity difference between the matrix

and disperse domain polymers was not large enough to make a difference in cell morphology. However, it is possible to control the degree of cell opening by adjusting the absolute value of the shear viscosity as well as the elongational viscosity of the disperse domain polymer to obtain foams with high expansion ratios and thin cell walls.

4.5. Acknowledgements

The authors are grateful to Dow Chemical Japan for providing PS and LLDPE and to Tosoh Corporation for providing HMS-PE and HDPE.

4.6. References

[1] R. H. Hansen, W. M. Martin, *J. Polym. Sci. Part B: Polym. Lett.* **1965**, *3*, 325.

[2] N. S. Ramesh, D. H. Rasmussen, G. A. Campbell, *Polym. Eng. Sci.* **1994**, *34*, 1685.

[3] N. S. Ramesh, D. H. Rasmussen, G. A. Campbell, *Polym. Eng. Sci.* **1994**, *34*, 1698.

[4] J. Shen, C. Zeng, J. Lee, *Polymer* **2005**, *46*, 5218.

[5] R. W. Sharudin, A. Nabil, K. Taki, M. Ohshima, *J. Appl. Polym. Sci.* **2011**, *119*, 1042.

[6] C.- M. Wong, S.- J. Tsai, C.- H. Ying, M.- L. Hung, *J. Cell. Plast* **2006**, *42*, 153.

Chapter 5

5.1. General Conclusion

In this dissertation, foamablity of polymer blends having non-homogeneity was observed in detail and the relation between several foam morphologies and material's mechanical properties obtained by rheological measurements was investigated. It was possible to modify open cell content (OCC), expansion ratios, bimodality of cell structure as well as cell sizes and cell densities by using Interpenetrating polymer Networks and blends made of two immiscible polymers. In the following, the detailed results of all studies are summarized.

In chapter 2, a solvent mixing process was applied to prepare polylactic acid ($P_{L,D}LA$)-polymethyl methacrylate (PMMA) and $P_{L,D}LA$-PS (polystyrene) blends with different weight ratios and different degrees of cross-linking for the formation of Semi-Interpenetrating Polymer Networks (Semi- IPNs). The samples were foamed during a physical batch foaming process using supercritical carbon dioxide. It was possible to modify the open cell content, the averaged cell size of the bubbles in the polymer matrix, and the cell density. Rheological investigations have shown that a local non-homogeneity, i.e. a partial miscibility of PMMA and PS in the $P_{L,D}LA$ matrix, caused harder and softer domains. The softer domains were ruptured during foaming whereas the harder domains could maintain the foam morphology without collapsing.

In chapter 3, the concept of exploiting non-homogeneity on the base of Semi-Interpenetrating Networks was extended and applied to the system PS-PMMA.

Contrary to the previous study, it was not necessary to use an additional solvent to mix the matrix polymer with monomers and cross-linking agent. The used polystyrene pellets could be dissolved homogeneously in methyl methacrylate monomers. An In-Situ process was applied to saturate the mixture with supercritical carbon dioxide, to polymerize and cross-link the methyl methacrylate in polystyrene, and to foam the blend eventually. Subsequent visual observations identified the PS matrix having large bubbles and cross-linked PMMA having small ones. A case study has shown that small bubbles definitely belonged to the cross-linked domains of PMMA.

In chapter 4, immiscible blends of amorphous polystyrene and three different types of polyethylene (PE) were prepared without using IPN structures. The polyethylene components had different melt flow indices (MFIs) and a comparative study of morphologies of foams prepared in a pressure-quench process was conducted. The foams were prepared at temperatures lower than glass transition of PS and melting temperature of PE, over glass transition of PS but with PE in the solid state, and over glass transition of PS and melting point of PE to study the influence of the MFIs on foam morphology. By adding PE in the range of low concentrations, a significant decrease of averaged cell size and homogeneous foam morphology could be observed; moreover, foams prepared at elevated temperatures have shown open cellular morphologies.

It was shown in the aforementioned sections that a diversity of different foam morphologies could be prepared by modifying the properties of the polymer sample, i.e., cross-linking and non-homogeneity through blending of immiscible components, without changing the foaming process. The investigated systems were used as model systems and the general principles presented in this thesis can be transferred to any

other system having similar properties. Thus, the possible applications can be related to porous materials for cell seeding in the field of tissue engineering, improvement of heat transfer properties for insulators as well as for utilizations in packaging industry.

5.2. List of Publications

D. Kohlhoff, M. Ohshima

Open Cell Microcellular Foams of Polylactic Acid (PLA) based Blends with Semi-Interpenetrating Polymer Networks

Macromol. Mater. Eng. **2011,** *296*, 770

D. Kohlhoff, N. Abacha, M. Ohshima

In-Situ Preparation of Cross-linked PS-PMMA Blend Foams with a Bimodal Cellular Structure

Polym. Advan. Technol. **2011**, *published online*

D. Kohlhoff, M. Ohshima

Influence of Polyethylene Disperse Domain on Cell Morphology of Polystyrene Based Blend Foams

J. Polym. Sci. B: Pol. Phys. (submitted; 25-07-2012)

5.3. International Conference

D. Kohlhoff, M. Ohshima

Open Cell Microcellular Foams of Polylactic Acid (PLA) based Blends with Semi-Interpenetrating Polymer Networks

Oral presentation, *ANTEC 2011*, Haynes Convention Center, Boston, Massachusetts USA, May 01-05.

5.4. Acknowledgements

The present thesis summarizes the results of research that has been carried out under the supervision of Professor Masahiro Ohshima at the Materials Process Engineering Division belonging to the Department of Chemical Engineering, Graduate School of Engineering, Kyoto University from October 2008 until September 2011.

At first, the author owes his deepest gratitude to Professor Masahiro Ohshima who accepted him as a doctoral course student at the Materials Process Engineering Division at Kyoto University and who supervised the present thesis during the last three years. This thesis would not have been possible without Professor Ohshima's continuous guidance, supervision, and encouragement throughout this work.

The author also would like to thank Professor Toshikazu Takigawa from the Department of Material Chemistry and Professor Ryoichi Yamamoto from the Department of Chemical Engineering of Kyoto University for their suggestions and careful examination of this thesis.

The author owes Dr. Shinsuke Nagamine and Dr. Kentaro Taki a debt of gratitude for their advices in conducting experiments, especially Dr. Kentaro Taki for his continuous help and his advices related to experimental procedures.

The author also thanks Dr. Shinsuke Nagamine and Dr. Jin-Woong Kim for their kind help related to finding an apartment, getting internet access, and to many other

difficulties in daily life.

The author is in acknowledgement of the scholarship of the Ministry of Education, Culture, Sports, Science & Technology (MEXT, Japan) for financial support during the last three years.

The author would like to express his deepest gratitude to all present and former students and members of the Materials Process Engineering Division for their help, their advices, and for spending a pleasant time together.

The author is indebted to Dr.-Ing. Ingmar Gerlach who gave helpful advices related to the application process for the International Doctoral Program and during the author's first months in Kyoto.

Deepest gratitude has to be expressed to all of the author's friends from all over the world.

The author would like to thank all colleagues and friends from BASF Polyurethanes, Lemförde plant for the extraordinarily pleasant situation at work.

Finally, the author expresses his deepest gratitude to his whole family and his fiancée Daiane for continuous support in good and bad times.